

## BVRI PHOTOMETRY OF STAR CLUSTERS IN THE BOK REGION OF THE LARGE MAGELLANIC CLOUD

GONZALO ALCAINO<sup>a),b),c)</sup> AND WILLIAM LILLER<sup>a),b)</sup>

Instituto Isaac Newton, Ministerio de Educación de Chile, Casilla 8-9, Correo 9, Santiago, Chile

Received 5 August 1986; revised 9 February 1987

### ABSTRACT

Photographic *BVRI* color-magnitude and color-color diagrams are provided for 14 star clusters situated in the Bok region of the Large Magellanic Cloud. Eleven have NGC numbers: 1834, 1836, 1839, 1847, 1850, 1854, 1856, 1858, 1860, 1863, 1870; the remaining three are from the SL (Shapley-Lindsay) catalog: 234, 237, and 304. None of these clusters have had previous stellar photometry in *R* and *I*, and only four of them in *B* and *V*. We have estimated the reddening for each cluster by fitting the main sequence of the CMDs to the unreddened ZAMS. Ages have been derived from the MS turnoff and from the brightest blue star following the method developed by Hodge (1983), and from fitting the CMDs to the isochrones of Maeder and Mermilliod (1981). All clusters are found to be young, with ages ranging from  $17 \pm 6 \times 10^6$  yr for NGC 1858 to  $90 \pm 30 \times 10^6$  yr for NGC 1860. They lie symmetrically in the center of the age histogram of galactic clusters (Lyngå 1982). Both distributions peak close to  $\log_t \sim 7.5$ .

### I. INTRODUCTION

One of the most fundamental characteristics of the star clusters in our galaxy is the distinct dichotomy between the very old massive globular clusters with ages greater than  $10^{10}$  yr, and very likely coeval around  $17 \pm 2 \times 10^9$  yr; and the less massive open clusters, younger than  $10^{10}$  yr, and situated in the galactic disk (Sandage 1982). This dichotomy does not seem to exist in the LMC, where "populous globular-like intermediate-age clusters" cover the gap between the old globulars such as NGC 2257 (Stryker 1983) and younger objects that resemble galactic open clusters in an age span from around  $10^6$  up to  $10 \times 10^9$  yr, the latter age being that of the open cluster NGC 188, which defines a lower bound to the age of the galactic disk (VandenBerg 1985).

It is, at present, difficult to compare from the literature the ages of clusters in the Magellanic Clouds, owing to the variety of ways in which authors have interpreted the observational data and the various theoretical models used. With these considerations in mind, and taking the advantage of the large field of the photographic plates of the 2.5 m telescope at CARSO-Las Campanas and the 3.6 m telescope at ESO, we have embarked on an investigation of LMC clusters within an area of 1 square degree. Because of its large concentration of clusters, we have chosen the so-called Bok region (Bok and Bok 1969), located in the northwestern part of the LMC bar. Its position is identified in Fig. 1 [Plate 30], and an enlargement of the studied area is shown in Fig. 2 [Plate 31]. As can be seen from Fig. 2, this zone is densely populated with clusters, the most conspicuous being NGC 1847, NGC 1850, NGC 1854, and NGC 1856. Fourteen clusters have been chosen for analysis in this study; they are listed in Table I.

In the color-magnitude diagram (CMD) of the integrated

*V* magnitudes and *B* – *V* colors for 147 LMC clusters (van den Bergh 1981), there exists a rich population of young blue clusters, and about one-fourth as many older red objects. Separating the two cluster groups is a conspicuous gap at  $0.3 < B - V < 0.7$ . As listed in Table I, eight of the 14 clusters considered here have integrated colors; all lie in the blue sector of the gap.

Color-magnitude diagrams in *BV* have been derived previously for four of our clusters; they are: NGC 1850 (Tifft and Connolly 1973; Robertson 1974), NGC 1854 (Robertson 1974; Connolly and Tifft 1977), NGC 1847 (Nelson and Hodge 1983), and NGC 1856 (Hodge and Lee 1984). Two *BV* photoelectric sequences in the field have been published: by Tifft and Snell (1971) for their photometric investigations into the nature of the LMC bar, and used in the calibration of the photographic plates taken for the CMD work on NGC 1850 and NGC 1854; and by Hodge and Lee (1984), who derived another sequence for calibration of the photographic plates used in their work on NGC 1847 and NGC 1856.

In concluding this section, we note that a field near the center of the Bok region was studied by Hardy *et al.* (1984), who carried out a photometric analysis of 18 000 stars. As we will see in Sec. IV, their main conclusion is that stellar formation continues in the LMC bar and that the bulk of star formation started between one and three billion years ago.

A preliminary report on the investigation presented here-in appears in IAU Symposium No. 108, *Structure and Evolution of the Magellanic Clouds* (van den Bergh and de Boer 1984).

### II. THE DATA

As noted in the previous section, photographic plates have been obtained with both the 2.5 m telescope at Las Campanas and the 3.6 m telescope at La Silla. Additional photographs were taken with the 1.5 m telescope at the Cerro Tololo Inter-American Observatory. The plates have been calibrated with a Bok region *BVRI* photoelectric sequence of 15 stars in the magnitude range  $9.4 < V < 15.3$  (Alcaino and Liller 1982). This sequence has been extended to fainter magnitudes using a Pickering-Racine wedge in the two larg-

<sup>a)</sup> Based on observations collected at the European Southern Observatory, La Silla, Chile.

<sup>b)</sup> Guest Investigator at Las Campanas Observatory, which is operated by the Carnegie Institution of Washington.

<sup>c)</sup> Visiting Astronomer, Cerro Tololo Inter-American Observatory, National Optical Astronomy Observatories, which is operated by The Association of Universities for Research in Astronomy, Inc., for the National Science Foundation.

TABLE I. Integrated-light data for star clusters studied in the LMC.

Cluster	V	B-V	U-B	Q	$\frac{\text{Age}}{V_B}$
1834	11.82	0.29	-0.32	-0.53	Y
1836	-	-	-	-	-
1839	-	-	-	-	-
1847	11.06	0.20	-0.33	-0.47	Y
1850	8.96	0.12	-0.35	-0.44	Y
1854	10.39	0.21	-0.22	-0.37	Y
1856	10.06	0.34	0.07	-0.17	I
1858	-	-0.20	-1.04	-0.90	VY
1860	11.04	0.14	-0.39	-0.49	Y
1863	10.98	0.16	-0.33	-0.45	Y
1870	11.26	0.19	-0.21	-0.35	Y
SL234	-	-	-	-	-
SL237	-	-	-	-	-
SL304	-	-	-	-	-

Data are from van den Bergh (1981).

er telescopes. A log of the photographic material is given in Table II.

In each cluster, we divided the stars into two areas: an inner circle, where the likelihood of membership (as well as the contamination) is higher; and an outer ring, in which, consequently, the contamination (and the probability of membership) is lower. In the CMDs, stars from the inner circles are represented as dark dots; light circles indicate stars from the outer rings.

The measurement of the photographic plates was carried out with the ESO Askania iris photometer. The raw magnitudes were then converted to true magnitudes using equations of the type:

$$V = v + \varepsilon(b - v) + \xi_1,$$

$$B - V = \mu(b - v) + \xi_2,$$

$$V - R = \eta(v - r) + \xi_3,$$

$$V - I = \chi(v - i) + \xi_4.$$

The values of the coefficients derived for the several telescopes that we employed are listed in Table III. The errors of the coefficients average less than  $\pm 0.010$ . Because the two infrared plates used were taken before the Pickering-Racine wedge for the triplet configuration was available at the 3.6 m ESO telescope, they could only be calibrated to the limit of the photoelectric sequence of  $I \sim 14$ . However, the  $I$  magni-

TABLE II. Log of the photographic plates.

Telescope	Plate Number	Date	Emulsion	Filter	Exposure (min)	Lim. Mag.
1.5-m Tololo	T 114	1-01-72	103aD	GG 14	3	17.0
	T 113	1-01-72	103aD	GG 14	7	17.5
	T 172	3-01-72	IIaO	GG 13	5	17.6
	T 171	3-01-72	IIaO	GG 13	15	17.9
2.5-m du Pont	D2057	7-11-81	103aD	GG495	30	17.5
	D2058	7-11-81	103aD	GG495	64	18.0
	D 123	4-01-78	103aO	GG385	40	19.0
	D 117	3-01-79	103aO	GG385	60	19.0
3.6-ESO	E 398	29-10-83	IIaD	GG495	5	19.0
	E 397	29-10-83	IIaD	GG495	12	19.2
	E 396	29-10-83	IIIaJ	GG385	5	19.2
	E 395	29-10-83	IIIaJ	GG385	12	20.0
	E 394	29-10-83	IIIaF	OG590	5	17.6
	E 392	29-10-83	IIIaF	OG590	5	17.6
	E 391	29-10-83	IIIaF	OG590	17	19.3
	E 390	29-10-83	IIIaF	OG590	17	19.3
	E 298	12-11-82	IVN	RG 9	10	14.5
	E 299	12-11-82	IVN	RG 9	10	14.5

All listed plates obtained with the 2.5-m du Pont telescope at Las Campanas and the 3.6-m telescope at La Silla have been taken with a Pickering-Racine wedge, with the exceptions of the I plates in the 3.6 m telescope. The plate scales from the different telescopes are as follows : 1.5-m Tololo 18.1 arc sec/mm, 2.5-m Campanas 10.8 arc sec/mm, 3.6-m ESO 13.6 arc sec/mm.

TABLE III. Coefficients of the magnitude equations.

Telescope	$\epsilon$	$\xi_1$	$\mu$	$\xi_2$	$\eta$	$\xi_3$	$\chi$	$\xi_4$
1.5 Tololo	0.03	-0.02	0.96	+0.04	-	-	-	-
2.5 Dupont	0.06	-0.03	0.91	+0.07	-	-	-	-
3.6 ESO	0.05	-0.02	1.15	-0.11	0.91	+0.03	1.00	0.00

tudes are especially useful in depicting the red star sequences. The standard deviations as a function of magnitude are shown in Fig. 3.

The summary of the results is given in Table IV. This table lists for each cluster the figure number for the finding chart; the sky area within each radius or annulus; the number of measured stars therein; the range of the measured visual magnitudes; the table numbers listing the magnitudes and colors, and the figure numbers of the corresponding color-magnitude and color-color plots. Table V summarizes the work of the other investigators who have carried out photometry on four of the clusters.

### III. THE RESULTS

From the *BVRI* photometric data summarized in Table IV, CMDs and color-color plots with  $B - V$ ,  $B - R$ ,  $V - I$ , and  $B - I$  baselines have been plotted. Four global features can be identified in the  $V$  vs  $B - V$  and  $V$  vs  $B - R$  CMDs: (1) the upper end of the cluster main sequence (MS); (2) somewhat brighter bluish stars, probably core-helium-burning blue giants and supergiants, at  $V \sim 14$  and  $B - V \sim 0.0$ ,  $B - R \sim 0.0$  in NGC 1850 and NGC 1854; (3) evolved red giants or supergiants to  $B - V \sim 2.0$  and  $B - R \sim 3.0$  in NGC 1850 and NGC 1854; (4) fainter cool giant-branch stars extending from an upper red tip of  $V \sim 16.5$  and

$B - V \sim 2.0$ ,  $B - R \sim 3.0$  to  $V \sim 19.0$ , and  $B - V \sim 1.0$ ,  $B - R \sim 1.3$  in NGC 1850 and NGC 1854. These last stars must be a part of the older population which is abundant in this part of the LMC (Hardy *et al.* 1984; Nelson and Hodge 1983; Hodge and Lee 1984). As can be seen, all these features stand out clearly in well-populated clusters like NGC 1850 and NGC 1854, but can hardly be discriminated in the stellar-deficient clusters NGC 1834, NGC 1860, SL 234, and SL 237.

In what follows, we have adopted the corrected distance modulus to the LMC of  $(m - M)_0 = 18.59$ , corresponding to a distance of 52.2 kpc (Sandage and Tammann 1974). However, we should caution that recently Schommer, Olszewski, and Aaronson (1984) carried out deep CCD photometry, and after measuring unevolved main-sequence stars for two LMC clusters, proposed a much smaller distance modulus of  $(m - M)_0 = 18.20 \pm 0.2$  corresponding to a distance of  $43.6 \pm 4$  kpc. A value of  $E(B - V) = 0.06 \pm 0.02$  is generally adopted towards the LMC including the old and intermediate-age star clusters (Sandage and Tammann 1974), but objects with ages  $< 3 \times 10^8$  yr are expected to be embedded in absorbing matter, which should strongly increase the reddening. As all the clusters studied here are blue, and therefore young, individual reddening must be derived for each object.

To estimate the reddening for each cluster, we fitted the measured main sequence to an unreddened zero-age main sequence (Mermilliod 1981). The reddening values derived in this way are listed in Table VI. Because the reddening line of  $E(V - R)/E(B - V) = 0.56$  (Taylor 1986) is practically parallel to the fiducial line of the  $V - R$  vs  $B - V$  color-color plots, as shown in the respective plots of NGC 1850 and NGC 1854 (Figs. 16 and 19), reddening could not be deduced from these diagrams.

In order to make a first estimation of the age, we have followed the procedure used by Hodge (1983). In his paper, Hodge comments on the difficulty of comparing ages of clusters in the Magellanic Clouds, owing to the variety of theoretical models used and ways to interpret the data. In order to homogenize the age data, he assembled the pertinent CMDs and compared them with a single set of theoretical predictions, using the isochrones of Schlesinger (1969), Stother (1972), and Brunish (1981). Hodge then age-dated the younger clusters with two indices: the magnitude of the MS turnoff, and the magnitude of the brightest blue ( $B - V < 0.4$ ) evolved star. In practice, the age of a young blue cluster, such as those in our sample, was determined first by locating the MS tip, which usually can be identified by an abrupt decrease in star density in the MS. Then, an independent value of age is obtained from the magnitude of the brightest blue star of the MS that is likely to be a cluster member. This star should mark the locus of recently evolved hot stars, their surface temperatures not having decreased

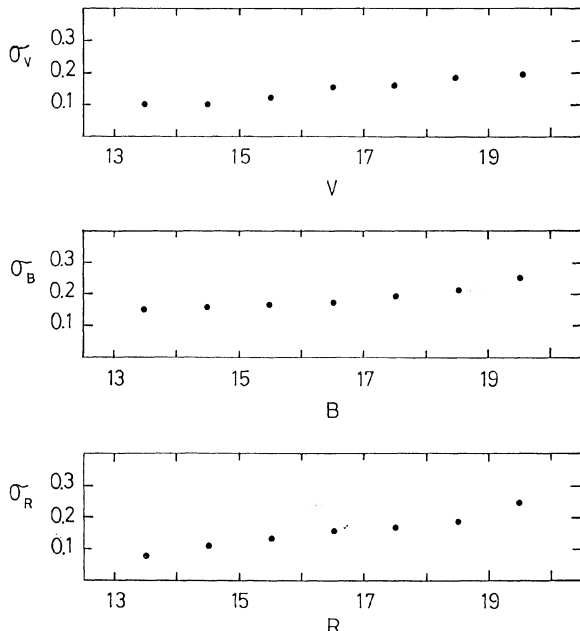


FIG. 3. Standard deviation as a function of magnitude.

TABLE IV. Summary of cluster results.

1 NGC	2 Fig. Cap.	3 Inner Radius	4 Outer Radius	5 No. Stars Col. 3	6 No. Stars Col. 4	7 <V< Range V Mag	8 Table Numbers	9 Fig.Cap. Plots
1834	3	0.43	0.67	10	16	14.2-19.4	8,9	21
1836	4	0.60	1.03	14	54	13.3-19.2	10,11	22
1839	5,6	0.85	1.21	38	27	13.5-18.5	12,13	23
1847	7,8	0.74	-	81	-	14.1-19.6	14	24
1850	9,10	1.52	2.07	87	130	13.6-19.4	15,16	25
1854	11,12	1.50	2.5	117	134	13.7-19.1	17,18	26
1856	13	0.71	1.17	-	104	16.2-19.6	19	27
1858	14	3.6	-	64	-	12.0-17.6	20,21	28
1860	15	0.54	0.85	13	10	16.4-19.0	22	29
1863	16	0.60	0.78	10	13	15.9-19.1	23	30
1870	17	0.63	-	22	-	14.9-18.6	24	31
SL234	18	0.57	-	16	-	14.9-18.3	25	32
SL237	19	0.68	1.76	15	10	12.2-17.1	26,27	33
SL304	20	0.67	1.32	39	42	15.1-19.4	28	34

Column 1 (C1) gives the cluster's NGC number or other name; (C2) the number of the figure captions of the finding charts; (C3) the radius in arc-min of the inner area measured in each cluster. These stars are indicated as full dots in the plots; (C4) the outer radius of the outer ring in arc-min measured in each cluster. These stars are indicated as circles in the plots; (C5) the number of stars measured in the inner radius; (C6) the number of stars measured in the outer ring; (C7) the range of visual magnitudes; (C8) the table numbers listing magnitudes and colors; (C9) the figure numbers listing the color-magnitude and color-color plots.

sufficiently to become red supergiants. Because the ages derived in this way are sensitive to the theoretical model used, as well as the difficulty in identifying the brightest MS blue star and the brightest MS star, Hodge concludes that in an absolute sense the ages could be incorrect by a factor of 2. The mean values obtained for our clusters by these two methods calibrated from Fig. 1 in Hodge's paper are listed in Table VI.

Another procedure that we have used to estimate the age is to fit our CMDs to the isochrones of Maeder and Mermilliod (1981). These isochrones given in the  $M_V$  vs  $(B-V)_0$  plane are calculated with  $X = 0.70$ ,  $Z = 0.03$ , with ages ranging from  $2.5 \times 10^7$  to  $6.3 \times 10^9$  yr for models with  $\alpha_c = 0$ . The value of metallic abundance is unknown for these clusters, but we believe that a metallicity around solar should represent a reasonable assumption for these blue objects. The isochrones have been superimposed on the  $V$  vs  $B-V$  diagrams using the apparent distance modulus for each cluster listed in Table VI. In the fitting of the isochrones, we weighted most heavily (1) dark circles (inner stars), and (2) the portion of the curves in the vicinity of the

"kink" near the top of the blue main sequence. However, the paucity of stars usually made it necessary to consider the entire range of colors. The deduction of the best age value from isochrone fitting, given in Table VI, includes what we feel are generous values for uncertainties which vary greatly depending on richness of clusters.

In deriving ages for these clusters, we have been guided by the recent work of others, especially Becker and Mathews (1983), who studied NGC 1866 in the LMC, Durand *et al.* (1984), who investigated two SMC clusters, Hodge and Lee (1984), who worked on NGC 1856, and Olszewski (1984), who studied NGC 1978. All of these investigators, as well as ourselves, were faced with the problem of field-star contamination, but it is reassuring to note that we find for NGC 1856 an age close to that found by Hodge and Lee. Similarly, the age found for the blue cluster NGC 1866 lies close to the ages we find for similarly colored clusters.

The weighted average of the two values also appears in Table VI. It is seen from the final column of Table VI that all the clusters are young, with ages ranging from  $17 \pm 6 \times 10^6$  yr for NGC 1858 ( $B-V = -0.20$ ) to  $90 \pm 30 \times 10^6$  yr for

TABLE V. Comparison with other authors.

1 NGC	2 Radius Meas.	3 No. Stars	4 Range of V	5 No. Stars in Common with this work	6 References of other authors
1847	0.74	283	13.1-20.0	81	Nelson and Hodge 1983
1850	2.7	158	13.6-18.0	62	Tifft and Connolly 1973
	2.8	105	14.2-16.5	6	Robertson 1974
1854	2.5	170	13.8-17.4	124	Connolly and Tifft 1977
	2.8	160	13..6-16.7	67	Robertson 1974
1856	1.17	273	14.3-20.6	104	Hodge and Lee 1984

TABLE VI. Reddening and ages for the clusters studied.

1 Cluster (NGC)	2 E(B-V)	3 (m-M) <sub>V</sub>	4 Mean Age MST+BBS 10 <sup>6</sup> y	5 Age isoch. 10 <sup>6</sup> y	6 Adopted Age 10 <sup>6</sup> y
1834	0.10:	18.89	52±20:	45±15	48±15
1836	0.20:	19.19	31±10	50±15	38±10
1839	0.27	19.40	22±8	45±10	33±8
1847	0.25	19.34	18±8	35±20	24±10
1850	0.18	19.13	19±10	24±6	21±5
1854	0.20	19.19	20±5	35±15	25±6
1856	0.26	19.37	66±18	90±50	73±20
1858	0.15	19.04	10±15	32±15	17±6
1860	0.18:	19.13	115±56	70±30	90±30
1863	0.20	19.19	57±20	60±20	58±17
1870	0.14	19.01	55±42	85±30	72±30
SL234	0.15:	19.04	57±22	40±20	48±20
SL237	0.17:	19.10	20±10	40±20	27±9
SL304	0.20	19.19	36±16	50±20	42±15

Column 1 (C1) lists the cluster name; (C2) gives the reddening which has been obtained by shifting the cluster main sequence to the unreddened ZAMS shown in the V vs B-V diagrams. Double dots mean estimated errors larger than  $\pm 0.03$ ; (C3) tabulates the apparent distance modulus  $(m-M)_V$  deduced by adopting the corrected distance modulus to the LMC of  $(m-M)_0 = 18.59$  (Sandage and Tammann 1974) and  $A_V = 3E(B-V)$ ; (C4) gives the mean age in millions of years, as obtained from the main sequence turnoff (MST) and the brightest blue star (BBS) calibrated in Fig. 4, following the method of Hodge (1983); standard deviations are the average of the two estimated errors of the two values; double dots represent values from only one of the two methods; (C5) lists our best age estimation in millions of years from the superimposed isochrones in the V vs B-V diagram, and the errors quoted are our estimates; (C6) tabulates our final adopted age in millions of years; the errors quoted on our own estimation, which we believe give a better representation than the standard deviation of the mean of columns 4 and 5.

NGC 1860. We should note that our CMDs could not be fitted to the recently improved isochrones for open clusters (VandenBerg 1985) since their youngest computed age,  $300 \times 10^6$  yr, is older than the age of the oldest cluster of our sample,  $90 \times 10^6$  yr.

Table VII lists the results for reddening and age deduced by the other authors for the four clusters observed in common. As can be seen, the values are in reasonable agreement with our deductions given in Table VI.

#### IV. DISCUSSION

The two major difficulties in determining the ages of LMC clusters arise from the rich contamination produced by the high background density in this region of the bar and from the extreme crowding in these distant and often compact clusters. Thus, less than 27 stars are measurable in six of the clusters, and only three have more than one hundred stars.

TABLE VII. Reddening and ages derived by other authors for the clusters observed in common.

1 Cluster NGC	2 Reddening E(B-V)	3 Age 10 <sup>6</sup> y Referenced Author	4 Age 10 <sup>6</sup> y Hodge(1983)	5 Reference
1847	-	25±10	16±4	Nelson and Hodge 1983
1850	0.13	30±10	40±10	Tifft and Connolly 1973
1854	0.23	25±15	30±10	Connolly and Tifft 1977
1856	0.18±0.05	80±30	120±20	Hodge and Lee 1984

Column 1 (C1) gives the cluster name; (C2) the reddening derived by the referenced author; (C3) the age in millions of years deduced by the referenced author; (C4) the age in millions of years derived by Hodge (1983) from the referenced CMDs following his method described here; (C5) reference to the other CMDs used in the deduction of these results.

Even on the short exposures, the brightest cluster members, often located near the cluster centers, are badly crowded and unmeasurable.

On the other hand, the upper main sequence of these young clusters should stand out clearly in their CMDs. In the CMD published by Hardy *et al.* (1984) for stars in the Bok region (the area they measured falls between NGC 1856 and NGC 1858), few LMC bar stars are found that have both  $(B - V) < 0.3$  and  $V < 17.0$ , corresponding approximately to  $(B - V)_0 < +0.1$  and  $M_V < -1.5$ . At redder colors we should expect more interlopers in our CMDs, bar stars that have evolved into the giant branch area of the CMD and that might reach  $V$  magnitudes of 17 or even 16 in a few isolated cases.

At the galactic latitude of the LMC ( $-33^\circ$ ) one ought to find about 1.9 galactic stars/arcmin<sup>2</sup> with  $V < 19$  (Allen 1973). Therefore, since the areas measured around the sparser clusters average no more than 3 arcmin<sup>2</sup>, we should encounter less than six galactic foreground stars per field, a third of these with  $B - V < 0.3$  (Allen 1973), and perhaps half of these too contaminated by cluster stars to measure.

However, in nearly all the cluster CMDs, we find stars, sometimes in large numbers, with  $0.2 < B - V < 1.5$  and  $V < 16$ . According to Maeder and Mermilliod (1981), only about 2% of the number of stars in the upper 2 mag of the hydrogen-burning main sequence should be found between the point of maximum temperature and the point of maximum brightness in  $M_V$ . They do not give figures for stars farther to the red, but, of course, they are observed, notably in the Hyades-Praesepe cluster group and the NGC 2281 group. However, these clusters are older, and evolution occurs more slowly. For the young LMC clusters, stars should be virtually absent from this rapid evolutionary phase of the isochrones.

It is thus difficult to explain why in NGC 1839, for example, there is a sizable group of stars in this prohibited zone (see Fig. 10). Inspection of the plates (Figs. 8 and 9) reveals no obvious selection effect, nor can one be easily invented. The offending stars in Fig. 10 tend to follow the young isochrones, but this may be a chance alignment. In the bar star CMD of nearly 18 000 stars made by Hardy *et al.* (1984), only four stars are found with  $V < 16.25$  and  $0.2 < (B - V) < 1.5$ ; in NGC 1839, there are ten in this zone. In all our diagrams where we have measured  $(B - V)$ s for a total of 922 stars, 130 (14%) lie in this "forbidden rectangle." In their calibration CMD, Hardy *et al.* do find 15 stars (out of 1500) in this rectangle, but still the number that we find is far less.

Having no other explanation for the existence of these yellow subsupergiants, we are forced to conclude, at least for the discussion that follows in this section, that they are, in fact, rapidly evolving stars which, for some reason, appear in substantial numbers in the clusters studied here. We also will ignore the possible existence of blue stragglers, which would confuse the situation hopelessly without further study.

With these points in mind, we comment here on the clusters individually:

**NGC 1834** (Figs. 4 [Plate 32] and 5; Tables VIII and IX). Many of the stars fainter than  $V = 17$  may be field stars, but the remainder can be considered as cluster members, leading us to feel secure in the age estimates given in Table VI. The apparent divergence from the theoretical main sequence of stars with  $V > 18.5$  will be seen to be characteristic of many of the clusters, and can be attributed to the presence of many

bar stars (Hardy *et al.* 1984). Fortunately, for most clusters, the derived value for the age depends negligibly upon the location of this part of the main sequence.

The  $V$ ,  $V - I$  diagram exhibits the selection effect set by the brighter magnitude limit of the  $I$  plates: red stars can be seen to fainter  $V$  magnitudes than the blue stars.

**NGC 1836** (Figs. 6 [Plate 33] and 7; Tables X and XI). We should be just beginning to see the upper main sequence of the cluster near  $V = 18$ . The spread in the magnitudes of the stars at the center of the diagram with  $V < 16.5$  suggests that stars evolve off the main sequence over a spread of some  $30 \times 10^6$  yr, comparable to the deduced age of the cluster.

**NGC 1839** (Figs. 8 and 9 [Plates 34 and 35], and 10; Tables XII and XIII). This CMD is better behaved in that the spread in  $V$  at intermediate colors is less pronounced than for the previous cluster, and the main sequence is well defined. The stars around  $V = 15$  have probably already begun their rapid evolution following hydrogen exhaustion.

**NGC 1847** (Figs. 11 and 12 [Plates 36 and 37], and 13; Table XIV). The four stars with  $V < 15$  indicate a young age, but it is possible that at least part of the apparent sequence running just below the isochrone labeled "50" is composed of cluster stars indicating a more advanced age. It almost seems as if there were two clusters present.

**NGC 1850** (Figs. 14 and 15 [Plates 38 and 39], and 16; Tables XV and XVI). The group of five blue stars near  $V = 14$  may be core-helium-burning giants that have begun their rapid evolution, suggesting that the blue kink may be even higher than Table VI implies. Possibly, the age of this cluster is close to  $10^7$  yr. A very similar  $BV$  CMD was published by Carney, Janes, and Flower (1985) for NGC 330 in the SMC.

**NGC 1854** (Figs. 17 and 18 [Plates 40 and 41], and 19; Tables XVII and XVIII). Again, a pair of stars near  $V = 14$  suggests that this cluster may also be very young. However, the most conspicuous characteristic of the  $BVR$  CMDs is the large number of stars falling inside the forbidden rectangle. As we noted above for NGC 1847, this might be indicative of a wide spread in ages of individual stars in the cluster. The  $V$ ,  $V - I$  diagram corresponds to those stars in the  $V$ ,  $B - V$  diagram lying above and to the right of the isochrone labeled "32."

**NGC 1856** (Figs. 20 [Plate 42] and 21; Table XIX). Only the outermost stars of this compact cluster could be measured, but the upper main sequence is well defined. However, owing to the greater age of this cluster, there is no clear distinction between the rapidly evolving stars at  $(B - V) > 0.7$  and the evolved bar stars.

**NGC 1858** (Figs. 22 [Plate 43] and 23; Tables XX and XXI). The two 12th magnitude stars both appear to be members indicating an age for the cluster of less than  $10^7$  yr, but the 20 stars in the prohibited rectangle argue for a more advanced age. The cluster is in a very crowded region.

**NGC 1860** (Figs. 24 [Plate 44] and 25; Table XXII). This sparse cluster lacks any luminous stars and thus must be considered to be the oldest of the group measured by us.

**NGC 1863** (Figs. 26 [Plate 45] and 27; Table XXIII). Likewise a sparse cluster, but still the main sequence is well defined. However, it is difficult to know where its tip is located.

**NGC 1870** (Figs. 28 [Plate 46] and 29; Table XXIV). Despite the few stars measured in this small cluster, a low age is suggested by the pair of stars near  $V = 15$ ,  $B - V = 0.2$ .

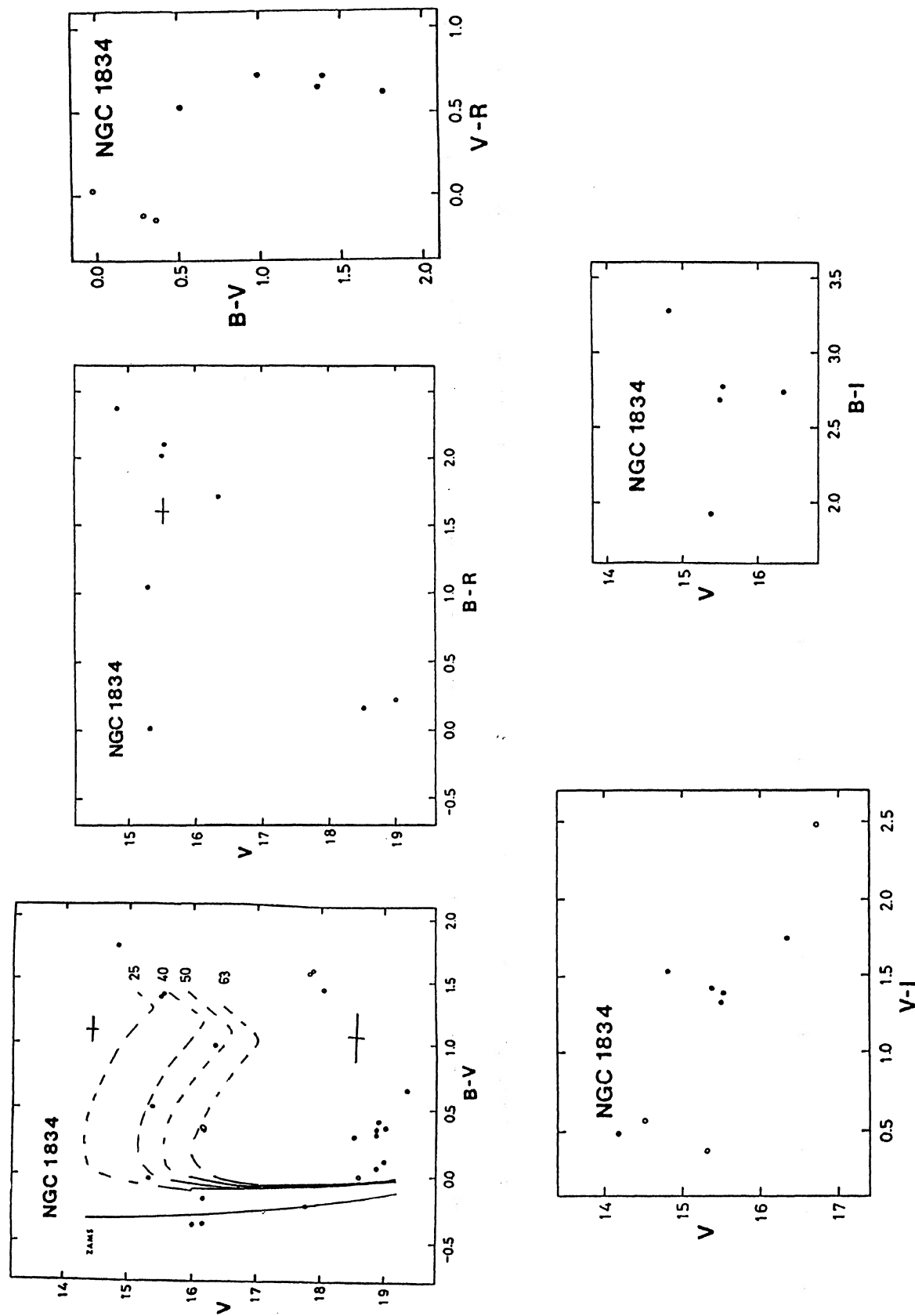


FIG. 5. Color-magnitude diagrams and color-color diagram of NGC 1834.

TABLE VIII. Photographic magnitudes and colors in NGC 1834.

Star	V	B-V	V-R	B-R
1	14.82	1.76	0.61	2.37
2	16.00	-0.37	-	-
3	16.35	0.99	0.72	1.71
4	18.87	0.35	-	-
5	16.17	-0.36	-	-
6	16.17	-0.17	-	-
7	15.39	0.51	0.53	1.04
8	14.19	-	0.43	-
9	15.53	1.39	0.71	2.10
10	15.50	1.36	0.65	2.01
11	15.32	-0.02	0.03	0.01
12	19.00	0.11	-	-
13	18.60	0.00	-	-
14	17.81	1.55	-	-
15	17.78	-0.23	-	-
16	18.03	1.42	-	-
17	19.35	0.65	-	-
18	18.90	0.41	-	-
19	16.72	-	0.93	-
20	19.00	0.36	-0.15	0.21
21	16.15	0.35	-	-
22	18.50	0.29	-0.13	0.16
23	17.86	1.57	-	-
24	18.87	0.06	-	-
25	18.89	0.31	-	-
26	14.51	-	0.30	-

TABLE IX. Photographic magnitudes and colors in NGC 1834.

Star	V	V-I	R-I	B-I
1	14.82	1.53	0.92	3.29
3	16.35	1.75	1.03	2.74
7	15.39	1.42	0.89	1.93
8	14.19	0.49	0.06	-
9	15.53	1.39	0.68	2.78
10	15.50	1.33	0.68	2.69
11	15.32	0.38	0.35	0.36
19	16.72	2.49	-	-
26	14.51	0.56	0.26	-

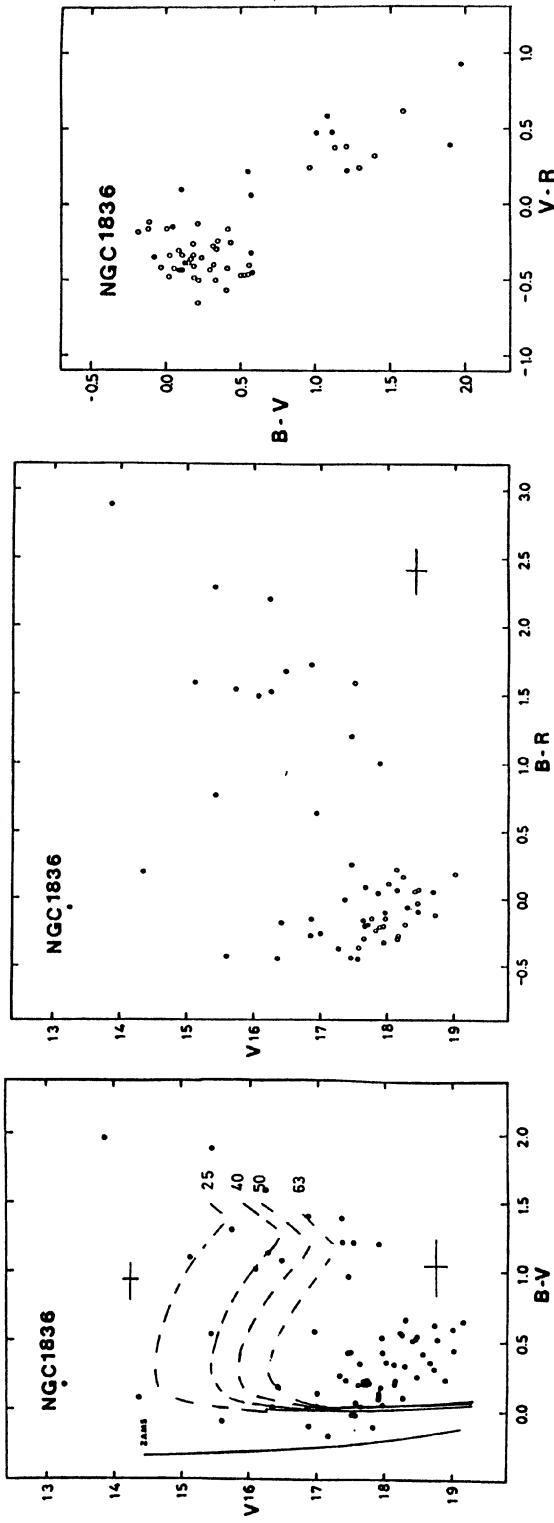


FIG. 7. Color-magnitude diagrams and color-color diagram of NGC 1836.

TABLE X. Photographic magnitudes and colors in NGC 1836.

Star	V	B-V	V-R	B-R
1	15.42	0.55	0.22	0.77
2	14.37	0.10	0.10	0.20
3	15.16	1.47	-	-
4	16.09	1.01	0.48	1.49
5	15.72	1.30	0.24	1.54
6	13.86	1.97	0.93	2.90
7	17.35	1.39	-	-
8	15.60	-0.08	-0.35	-0.43
9	17.90	1.21	0.21	1.00
10	16.97	0.57	0.07	0.64
11	16.28	1.14	0.38	1.52
12	17.00	0.13	-0.39	-0.26
13	17.96	0.05	-0.15	-0.10
14	15.41	1.90	0.39	2.29
15	19.01	0.44	-0.26	0.18
16	17.76	0.19	-	-
17	17.48	0.42	-0.17	0.25
18	16.35	0.03	-0.48	-0.45
19	18.44	0.51	-0.47	-0.04
20	16.25	1.59	0.61	2.20
21	13.27	0.19	-0.26	-0.07
22	16.86	-0.11	-0.17	-0.28
23	15.11	1.11	0.48	1.59
24	17.63	0.04	-0.34	-0.30
25	16.87	1.40	0.32	1.72
26	16.12	-	0.30	-
27	17.67	0.19	-0.40	-0.21
28	17.59	-0.04	-	-
29	18.27	0.10	-0.30	-0.20
30	18.55	0.42	-	-
31	17.36	0.42	-0.43	-0.01
32	17.45	0.96	0.24	1.20
33	17.52	1.21	0.38	1.59
34	17.68	0.21	-0.13	0.08
35	18.46	0.25	-0.35	-0.10
36	19.15	0.65	-	-
37	18.66	0.35	-0.30	0.05
38	17.57	0.06	-0.42	-0.36
39	17.97	0.42	-0.57	-0.15
40	17.53	-0.03	-0.42	-0.45
41	17.82	-0.11	-0.13	-0.24
42	17.43	0.22	-0.65	-0.43
43	12.15	0.22	-0.50	-0.28
44	16.85	0.01	-0.17	-0.16
45	16.41	0.17	-0.36	-0.19
46	17.76	0.19	-0.34	-0.15
47	18.01	0.35	-0.24	0.11
48	17.63	0.34	-0.50	-0.16
49	18.89	0.22	-	-
50	18.24	0.55	-	-
51	19.00	0.59	-	-
52	18.14	0.19	-0.49	-0.30
53	17.92	0.12	-0.34	-0.22
54	18.79	0.51	-	-
55	18.30	0.66	-	-
56	18.30	0.33	-0.40	-0.07
57	18.71	0.30	-0.43	-0.13
58	17.93	0.13	-	-
59	18.42	0.51	-0.46	0.05
60	18.14	0.34	-0.28	0.06
61	18.23	0.56	-0.40	0.16
62	17.16	-0.19	-0.18	-0.37
63	17.95	0.10	-0.43	-0.33
64	17.92	0.17	-0.39	-0.22
65	18.72	0.63	-	-
66	18.48	0.53	-0.46	0.07
67	17.65	0.18	-0.38	-0.20
68	17.37	0.25	-	-

TABLE XI. Photographic magnitudes and colors in NGC 1836.

Star	V	V-I	R-I	B-I
1	15.40	0.52	0.30	1.08
2	14.37	0.15	0.05	0.24
5	15.11	1.09	0.61	2.24
6	13.86	1.89	0.96	3.93

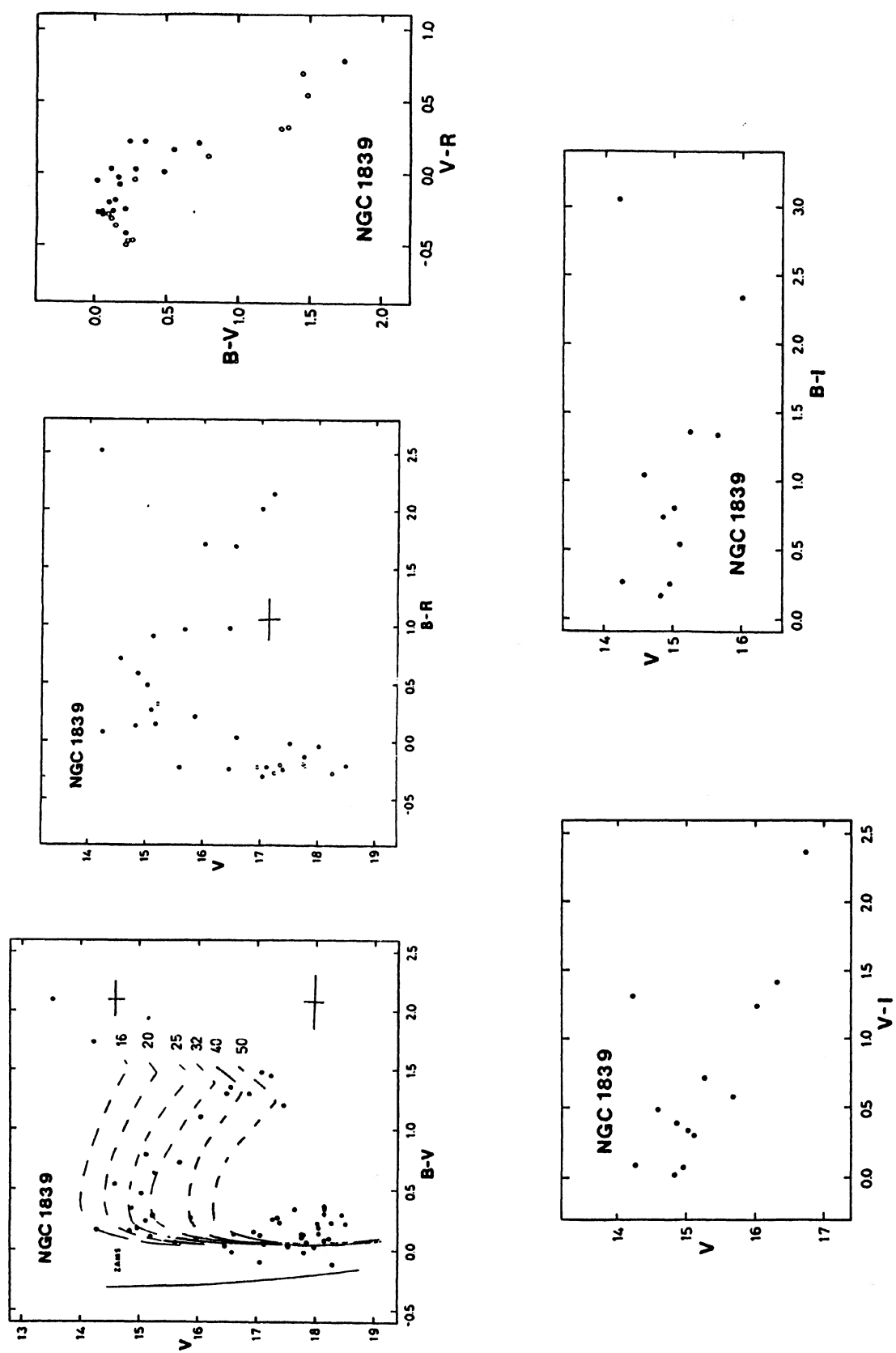


FIG. 10. Color-magnitude diagrams and color-color diagram of NGC 1839.

TABLE XII. Photographic magnitudes and colors in NGC 1839.

Star	V	B-V	V-R	B-R
1	16.58	-0.01	-	-
2	14.96	0.18	-	-
3	14.86	0.35	0.23	0.58
4	15.19	0.11	0.04	0.15
5	15.02	0.47	0.01	0.48
6	14.82	0.16	-0.02	0.14
7	15.10	0.24	0.23	0.47
8	15.26	0.64	-	-
9	17.24	1.45	0.70	2.15
10	14.22	1.74	0.79	2.53
11	15.68	0.73	0.22	0.95
12	14.58	0.55	0.16	0.71
13	14.26	0.17	-0.08	0.09
14	13.51	2.10	-	-
15	18.51	0.22	-0.42	-0.20
16	18.44	0.29	-	-
17	18.05	0.14	-	-
18	18.13	0.09	-	-
19	16.60	0.14	-0.18	0.04
20	17.45	1.20	-	-
21	17.57	-	-0.47	-
22	16.86	1.30	-	-
23	17.64	0.34	-	-
24	17.62	-	-0.37	-
25	15.60	0.06	-0.29	-0.23
26	18.29	-0.11	-	-
27	17.05	-0.10	-0.20	-0.30
28	16.66	-	-0.37	-
29	18.14	0.30	-	-
30	15.98	0.10	-	-
31	17.11	0.05	-0.27	-0.22
32	17.94	-	-0.42	-
33	16.45	0.03	-0.27	-0.24
34	18.05	0.19	-	-
35	17.79	0.13	-0.26	-0.13
36	17.97	0.03	-	-
37	18.02	0.21	-0.25	-0.04
38	17.51	0.03	-0.05	-0.02
39	17.26	0.25	-0.52	-0.27
40	18.26	0.23	-0.50	-0.27
41	18.19	0.35	-	-
42	17.09	-	0.06	-
43	16.13	-	-0.40	-
44	17.77	0.10	-0.29	-0.19
45	17.06	1.48	0.55	2.03
46	17.89	-	-0.37	-
47	17.06	0.13	-	-
48	18.22	0.10	-	-
49	17.79	0.12	-0.32	-0.20
50	18.15	0.37	-	-
51	17.80	-0.03	-	-
52	16.31	-	0.59	-
53	15.87	0.27	-0.04	0.23
54	16.47	1.30	0.32	1.62
55	16.83	-	0.44	-
56	16.95	0.15	-0.36	-0.21
57	17.40	0.23	-0.47	-0.24
58	17.34	0.26	-0.46	-0.20
59	16.01	1.10	0.62	1.72
60	15.22	0.29	0.03	0.32
61	16.77	-	-0.36	-
62	17.85	0.06	-	-
63	15.11	0.79	0.13	0.92
64	16.56	1.35	0.34	1.69

TABLE XIII. Photographic magnitudes and colors in NGC 1839.

Star	V	V-I	R-I	B-I
2	14.96	0.07	-	0.25
3	14.86	0.38	0.15	0.73
5	15.02	0.33	0.32	0.80
6	14.82	0.02	0.04	0.18
7	15.10	0.30	0.07	0.54
8	15.26	0.71	-	1.35
52	16.31	1.41	0.82	-
10	14.22	1.31	0.52	3.05
11	15.68	0.59	0.37	1.32
12	14.58	0.49	0.33	1.04
13	14.26	0.09	0.17	0.26
15	16.01	1.24	0.62	2.34
65	16.73	2.36	-	-

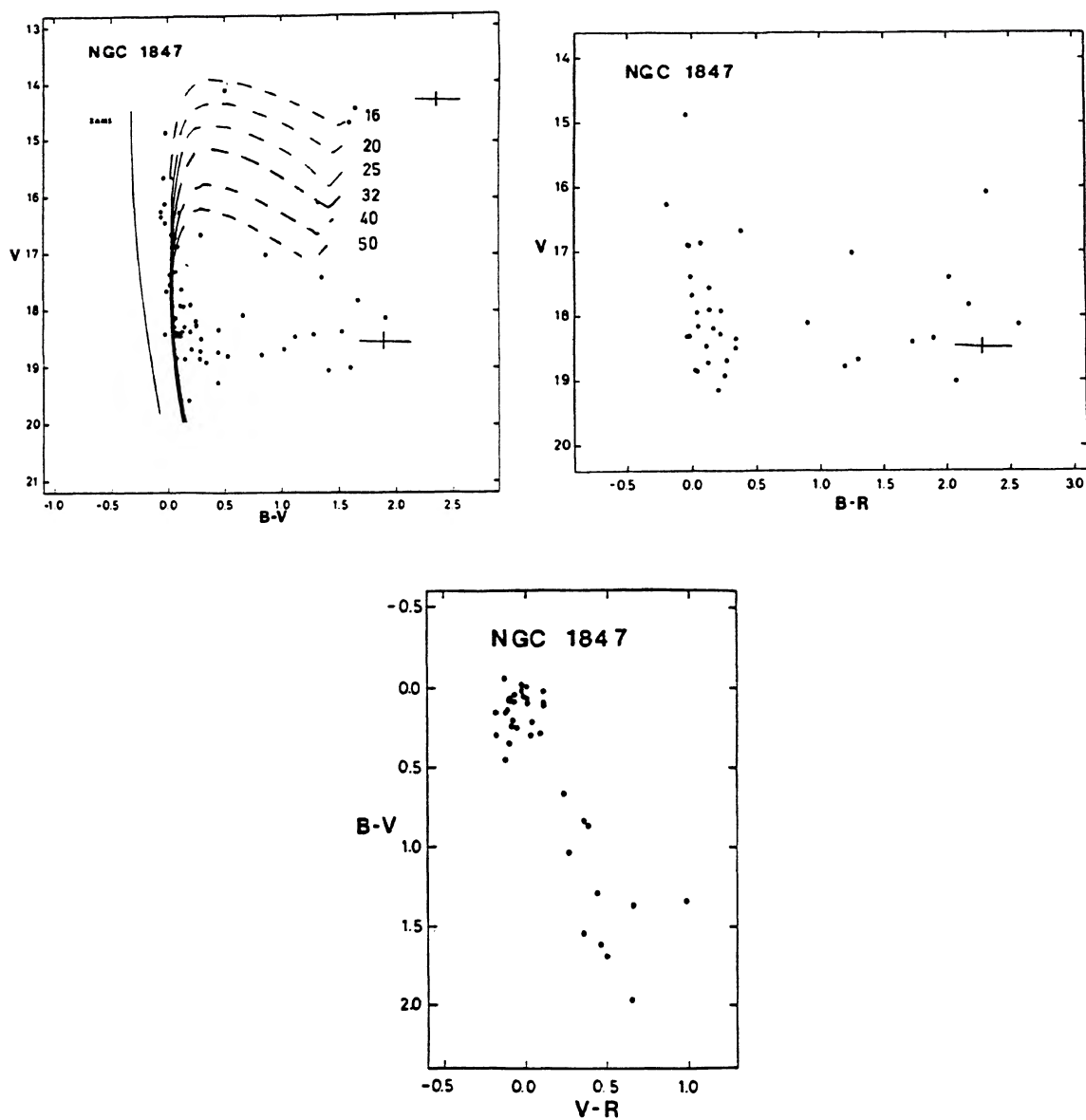


FIG. 13. Color-magnitude diagrams and color-color diagram of NGC 1847.

TABLE XIV. Photographic magnitudes and colors in NGC 1847.

Star	V	B-V	V-R	B-R
1	16.33	-0.06	-	-
2	16.58	-0.04	-	-
3	14.41	1.65	-	-
4	16.09	1.33	0.99	2.32
5	14.87	-0.02	-0.03	-0.05
6	16.73	0.06	-	-
7	16.11	-0.03	-	-
8	17.94	0.14	-0.10	0.04
9	18.28	0.25	-0.04	0.21
10	18.92	0.34	-0.09	0.25
11	18.14	1.92	0.65	2.57
12	18.39	-	-0.04	-
13	18.00	-	-0.16	-
14	18.15	0.07	-	-
15	17.90	0.20	-0.07	0.13
16	17.02	0.86	0.39	1.25
17	17.66	-0.01	0.01	0.00
18	16.99	-	-0.32	-
19	18.86	0.15	-0.11	0.04
20	16.44	-0.03	-	-
21	18.39	0.12	-	-
22	18.30	0.15	-0.17	-0.02
23	18.58	-	0.37	-
24	17.41	1.36	0.66	2.02
25	18.69	1.03	0.27	1.30
26	16.89	0.04	-0.06	-0.02
27	19.19	-	0.16	-
28	18.30	0.06	-0.09	-0.03
29	16.27	-0.06	-0.13	-0.19
30	17.75	-	-0.04	-
31	18.19	0.05	-0.01	0.04
32	18.45	0.12	-	-
33	18.46	1.13	-	-
34	18.42	-0.02	-	-
35	18.47	0.09	0.02	0.11
36	18.84	0.08	-0.06	0.02
37	18.85	0.28	-	-
38	19.07	1.42	-	-
39	18.41	1.29	0.44	1.73
40	18.85	-	0.35	-
41	18.77	-	0.46	-
42	17.26	-	0.00	-
43	18.38	0.20	-	-
44	19.59	0.19	-	-
45	18.50	0.30	0.04	0.34
46	18.69	-	0.47	-
47	16.66	0.28	0.10	0.38
48	19.21	-	0.29	-
49	18.83	-	-0.01	-
50	17.33	0.06	-	-
51	18.96	-	0.32	-
52	18.39	0.08	-	-
53	16.68	0.02	-	-
54	16.29	0.10	-	-
55	14.11	0.50	-	-
56	18.81	0.53	-	-
57	18.10	0.66	0.24	0.90
58	18.72	-	0.13	-
59	14.66	1.60	-	-
60	17.60	-	0.37	-
61	17.38	0.01	-0.02	-0.01
62	17.55	0.02	0.11	0.13
63	16.89	0.07	-0.09	-0.02
64	18.35	0.45	-0.11	0.34
65	19.03	-	0.25	-
66	17.61	-	0.47	-
67	17.91	0.11	0.11	0.22
68	16.87	0.06	0.01	0.07
69	18.86	-	-0.13	-
70	16.57	-	-0.01	-
71	18.79	0.83	0.36	1.19
72	18.72	0.29	-0.17	0.12
73	19.29	0.45	-	-
74	17.83	1.68	0.50	2.18
75	18.75	0.45	-	-
76	18.69	0.21	0.05	0.26
77	19.01	1.61	0.46	2.07
78	17.64	0.12	-	-
79	18.38	1.54	0.36	1.90
80	18.19	0.24	-0.08	0.16
81	19.15	0.09	0.11	0.20

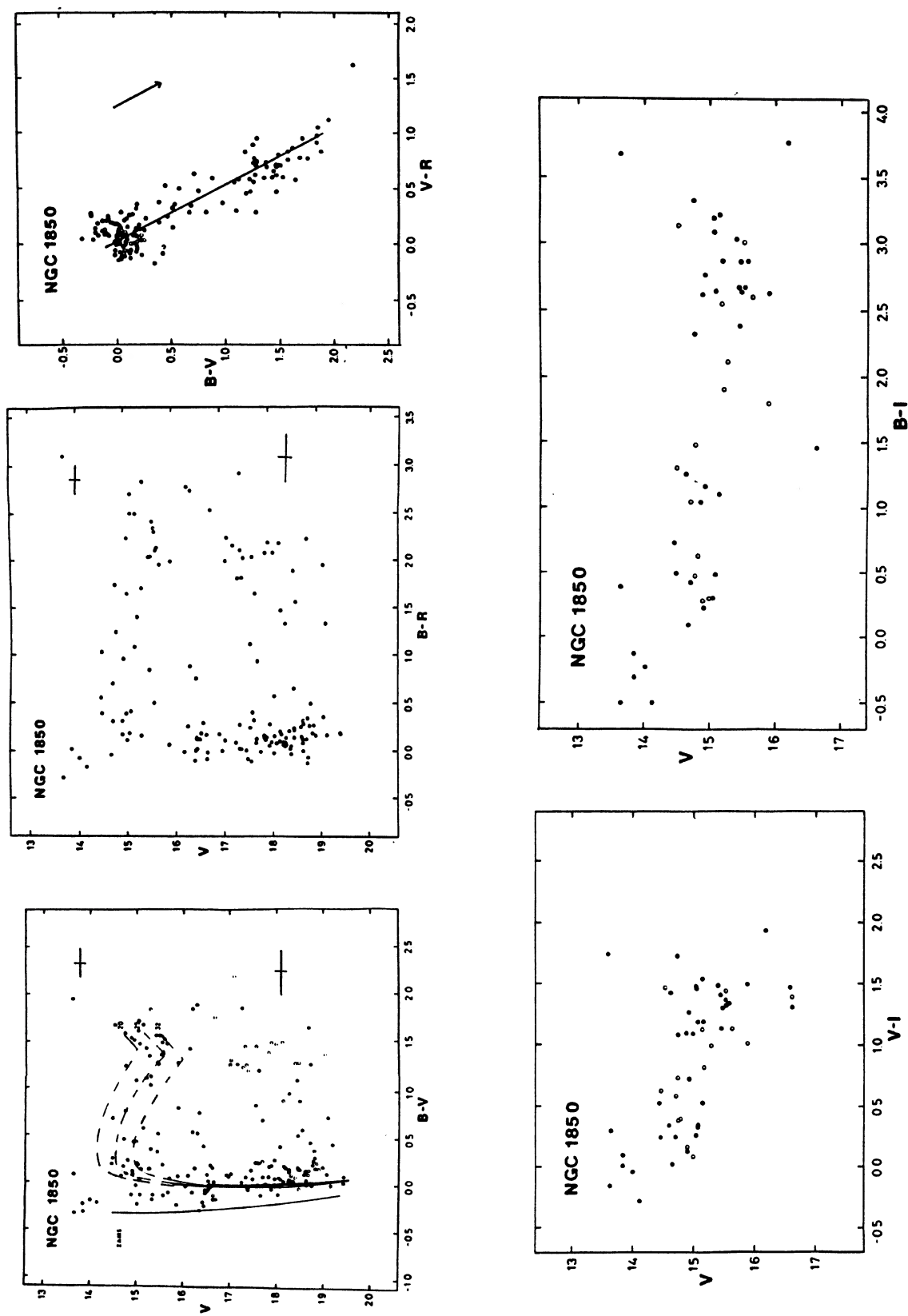


FIG. 16. Color-magnitude diagrams and color-color diagram of NGC 1850.

TABLE XV. Photographic magnitudes and colors in NGC 1850.

Star	V	B-V	V-R	B-R	Star	V	B-V	V-R	B-R
1	16.59	-	0.43	-	90	15.16	1.43	-	-
2	14.99	-	0.67	-	91	15.92	-	0.26	-
3	16.61	0.16	-	-	92	15.89	0.79	-	-
4	15.88	0.07	-0.01	0.06	93	16.61	-	1.22	-
5	15.70	0.05	-	-	94	16.18	0.54	-	-
6	17.86	-	0.04	-	95	16.44	-0.24	0.25	0.01
7	15.00	-0.23	-	-	96	16.63	0.02	0.14	0.16
8	14.66	0.07	-0.11	-0.04	97	15.29	0.35	-0.19	0.16
9	15.26	0.15	-	-	98	14.90	0.12	0.05	0.17
10	15.06	1.61	0.86	2.47	99	14.77	0.09	-	-
11	15.16	-	-	-	100	15.64	1.47	0.47	1.94
12	15.45	1.26	0.77	2.03	101	14.70	0.46	0.24	0.70
13	14.73	1.24	0.47	1.71	102	15.28	1.84	0.97	2.81
14	15.28	0.15	-	-	103	15.51	1.57	0.75	2.32
15	15.54	1.49	0.80	2.29	104	14.80	0.24	-	-
16	16.14	1.42	-	-	105	16.47	-0.08	0.21	0.13
17	15.14	0.58	0.49	1.07	106	16.47	-0.08	0.21	0.13
18	14.74	1.59	-	-	107	15.19	1.10	0.29	1.39
19	15.89	1.27	0.71	1.98	108	14.75	0.75	0.47	1.22
20	14.61	-	0.95	-	109	18.40	1.26	0.62	1.88
21	15.05	1.71	0.96	2.67	110	18.25	0.96	0.36	1.32
22	15.03	0.19	-	-	111	18.41	1.10	-	-
23	16.10	0.08	-	-	112	18.25	0.04	-	-
24	13.83	-0.23	0.24	0.01	113	18.63	0.10	0.01	0.11
25	15.40	1.56	-	-	114	18.60	0.14	0.00	0.14
26	13.64	0.09	-	-	115	17.01	1.29	0.94	2.23
27	15.35	-0.12	-	-	116	18.39	0.06	-0.09	-0.03
28	15.27	1.34	-	-	117	16.98	0.07	-0.07	0.00
29	16.04	-0.03	-	-	118	18.43	0.51	0.14	0.65
30	15.57	-0.13	-	-	119	18.59	0.10	0.15	0.25
31	15.85	-0.23	-	-	120	18.68	1.64	0.58	2.22
32	14.97	-0.03	-	-	121	17.00	1.25	0.73	1.98
33	13.84	-0.31	-	-	122	17.53	0.82	0.28	1.10
34	16.19	1.84	0.91	2.75	123	18.65	0.14	-	-
35	14.00	-0.19	0.11	-0.08	124	17.95	0.05	0.00	0.05
36	14.13	-0.21	0.03	-0.18	125	19.41	0.01	0.18	0.19
37	14.93	1.51	0.70	2.21	126	17.01	0.10	0.01	0.11
38	15.34	-0.18	-	-	127	17.65	-0.13	0.20	0.07
39	14.89	-0.13	-	-	128	19.14	-0.01	0.17	0.16
40	14.46	0.26	0.13	0.39	129	18.71	0.02	-0.15	-0.13
41	14.89	1.53	-	-	130	17.43	0.14	-0.14	0.00
42	15.07	1.47	-	-	131	17.83	-	-0.22	-
43	16.52	-0.08	0.20	0.12	132	18.05	-0.02	0.17	0.15
44	14.90	0.09	0.22	0.31	133	17.84	0.18	-0.06	0.12
45	15.47	1.56	0.83	2.39	134	16.64	-0.13	0.11	-0.02
46	16.34	-0.29	-	-	135	17.83	0.02	0.12	0.14
47	15.08	0.15	0.26	0.41	136	17.61	0.21	0.11	0.32
48	14.45	0.20	0.35	0.55	137	18.61	0.12	-0.04	0.08
49	15.59	1.52	0.60	2.12	138	18.03	0.39	0.18	0.57
50	15.15	1.68	0.78	2.46	139	17.68	0.23	-0.10	0.13
51	15.04	0.04	0.14	0.18	140	17.56	1.44	0.59	2.03
52	16.24	0.16	0.10	0.26	141	18.44	0.17	0.07	0.24
53	16.33	-	0.14	-	142	17.75	0.00	-0.01	-0.01
54	13.62	1.95	1.12	3.07	143	18.89	0.16	0.00	0.16
55	15.44	0.33	-	-	144	18.45	0.15	0.07	0.22
56	15.57	1.39	-	-	145	18.63	0.09	0.03	0.12
57	15.29	1.03	-	-	146	18.49	0.15	-	-
58	16.32	0.75	-	-	147	18.13	0.88	0.58	1.46
59	15.55	0.19	0.31	0.50	148	18.78	0.35	-	-
60	14.91	0.44	0.51	0.95	149	18.14	0.03	0.07	0.10
61	15.53	1.36	0.73	2.09	150	18.60	-	-0.05	-
62	13.64	-0.33	0.04	-0.29	151	19.02	-	0.01	-
63	15.43	1.27	0.74	2.01	152	18.84	0.22	0.05	0.27
64	14.60	-	0.12	-	153	18.27	0.14	-0.06	0.08
65	14.70	0.17	0.14	0.31	154	18.75	0.20	-	-
66	15.08	-0.13	-	-	155	18.63	-0.01	0.01	0.00
67	16.16	-	0.32	-	156	19.41	0.08	0.10	0.18
68	17.56	-	0.00	-	157	18.71	0.43	-0.09	0.34
69	16.50	0.09	-	-	158	18.53	0.57	-	-
70	17.89	0.19	-0.05	0.14	159	17.95	0.25	0.03	0.28
71	17.87	-0.06	-	-	160	17.31	1.44	0.65	2.09
72	16.65	-0.17	0.08	-0.09	161	18.72	1.25	-	-
73	17.59	-0.01	-0.10	-0.11	162	18.86	-	0.11	-
74	16.58	-0.04	-	-	163	17.24	0.01	0.08	0.09
75	17.27	1.85	1.05	2.90	164	18.00	-	-0.07	-
76	17.81	0.07	0.09	0.16	165	18.28	0.03	0.02	0.05
77	18.11	-0.02	-	-	166	18.07	0.05	0.03	0.08
78	17.67	-	0.15	-	167	17.59	0.22	0.18	0.40
79	17.53	0.22	0.03	0.25	168	17.98	1.46	0.61	2.07
80	14.97	1.08	0.55	1.63	169	16.29	1.88	0.83	2.71
81	16.40	-0.20	0.10	-0.10	170	18.80	0.27	0.22	0.49
82	17.61	1.19	0.45	1.64	171	19.03	1.35	0.59	1.94
83	18.73	-0.02	-0.06	-0.08	172	18.46	-0.05	0.19	0.14
84	19.05	0.11	0.25	0.36	173	18.34	0.03	0.18	0.21
85	18.70	-	-0.07	-	174	18.61	0.04	0.28	0.32
86	16.28	0.53	0.35	0.88	175	18.11	1.48	0.70	2.18
87	16.18	-0.10	0.08	-0.02	176	14.47	0.67	0.34	1.01
88	16.68	-0.18	0.17	-0.01	177	15.27	1.12	0.57	1.69
89	16.45	-0.11	0.13	0.02	178	17.38	-0.06	0.08	0.02

TABLE XV. (continued)

Star	V	B-V	V-R	B-R	Star	V	B-V	V-R	B-R
179	17.39	1.18	0.83	2.01	199	16.91	0.09	0.08	0.17
180	18.70	0.07	0.06	0.13	200	18.77	0.24	0.04	0.28
181	18.98	0.18	-	-	201	17.34	1.25	0.55	1.80
182	17.36	-0.05	0.06	0.01	202	18.21	0.19	-0.03	0.16
183	16.58	0.20	0.08	0.28	203	18.29	0.09	-0.01	0.08
184	18.14	0.19	0.01	0.20	204	18.45	1.27	0.28	1.55
185	16.68	1.75	0.76	2.51	205	17.48	0.05	-0.14	-0.09
186	18.49	0.88	-	-	206	15.44	0.52	0.31	0.83
187	17.10	2.18	1.62	3.80	207	17.99	-0.02	0.10	0.08
188	18.01	-0.11	-	-	208	18.03	0.06	-0.09	-0.03
189	17.68	0.67	0.27	0.94	209	17.33	0.07	0.20	0.27
190	18.37	0.00	0.05	0.05	210	17.27	1.22	0.58	1.80
191	16.53	0.02	0.16	0.18	211	17.15	1.25	0.89	2.14
192	19.09	0.71	0.62	1.33	212	19.19	0.42	-	-
193	18.27	0.03	0.11	0.14	213	17.83	1.38	0.69	2.07
194	14.52	1.67	-	-	214	18.69	-	0.08	-
195	15.67	-0.10	-	-	215	17.89	1.48	0.70	2.18
196	15.00	0.21	-0.10	0.11	216	18.82	0.15	0.03	0.18
197	16.41	0.39	0.36	0.75	217	14.98	0.43	-0.04	0.39
198	18.25	0.12	-0.06	0.06					

TABLE XVI. Photographic magnitudes and colors in NGC 1850.

Star	V	V-I	R-I	B-I
1	16.59	1.46	1.03	-
2	14.99	1.09	0.42	-
3	16.61	1.30	-	1.46
8	14.66	0.02	0.13	0.09
10	15.06	1.48	0.62	3.09
11	15.16	1.18	-	-
12	15.45	1.13	0.36	2.39
13	14.73	1.07	0.60	2.31
15	15.54	1.15	0.35	2.64
17	15.14	0.52	0.03	1.10
18	14.74	1.73	-	3.32
19	15.89	1.36	0.65	2.63
20	14.61	1.42	0.47	-
21	15.05	1.48	0.52	3.19
24	13.83	0.09	-0.15	-0.14
25	15.40	1.48	-	3.04
26	13.64	0.29	-	0.38
33	13.84	0.00	-	-0.31
34	16.19	1.93	1.02	3.77
35	14.00	-0.05	-0.16	-0.24
36	14.13	-0.29	-0.32	-0.50
37	14.93	1.26	0.56	2.77
40	14.46	0.24	0.11	0.50
41	14.89	1.10	-	2.63
42	15.07	1.18	-	2.65
44	14.90	0.12	-0.10	0.21
45	15.47	1.30	0.47	2.86
47	15.08	0.33	0.07	0.48
48	14.45	0.52	0.17	0.72
49	15.59	1.34	0.74	2.86
50	15.15	1.54	0.76	3.22
51	15.04	0.25	0.11	0.29
54	13.62	1.74	0.62	3.69
60	14.91	0.71	0.20	1.15
61	15.53	1.33	0.60	2.69
62	13.64	-0.17	-0.21	-0.50
63	15.43	1.40	0.66	2.67
64	14.60	0.33	0.21	-
65	14.70	0.24	0.10	0.41
90	15.16	1.12	-	2.55
92	15.89	1.00	-	1.79
93	16.61	1.40	0.18	-
98	14.90	0.15	0.10	0.27
99	14.77	0.37	-	0.46
100	15.64	1.13	0.66	2.60
101	14.70	0.58	0.34	1.04
103	15.51	1.43	0.68	3.00
104	14.80	0.38	-	0.62
107	15.19	0.81	0.52	1.91
108	14.75	0.72	0.25	1.47
176	14.47	0.62	0.28	1.29
177	15.27	0.99	0.42	2.11
194	14.52	1.46	-	3.13
196	15.00	0.08	0.18	0.29

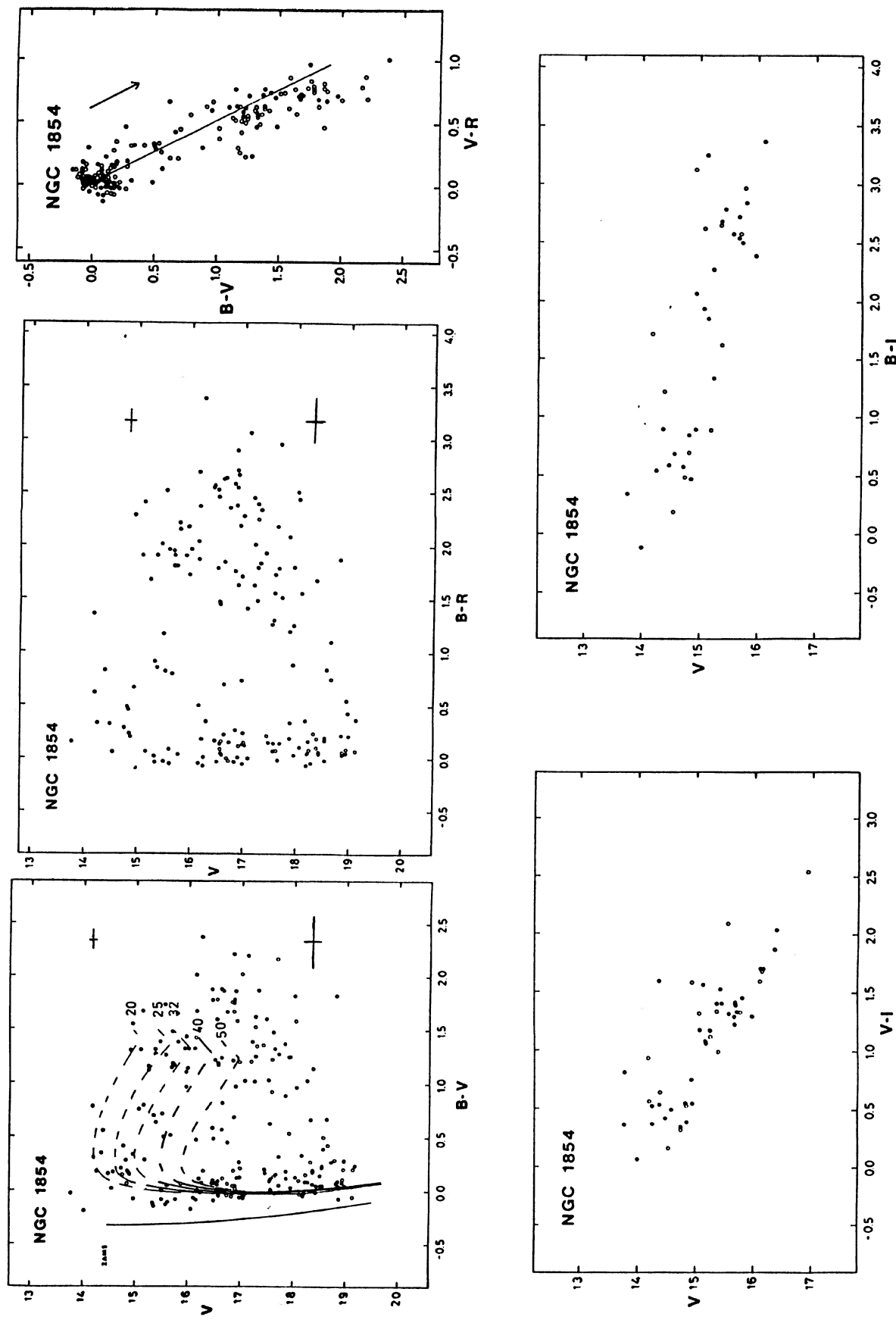


FIG. 19. Color-magnitude diagrams and color-color diagram of NGC 1854.

TABLE XVII. Photographic magnitudes and colors in NGC 1854.

Star	V	B-V	V-R	B-R
1	15.17	0.29	-	-
2	14.91	1.31	-	-
3	14.37	0.35	-	-
4	14.00	-0.19	-	-
5	14.58	0.18	-	-
6	15.07	0.76	-	-
7	14.72	0.21	-	-
8	15.67	-	0.75	-
9	15.38	1.28	0.78	-
10	13.75	-	-	-
11	14.37	-	-	-
12	15.15	0.80	-	-
13	15.24	1.16	-	-
14	14.25	-	-	-
15	16.04	-0.18	-	-
16	15.59	-0.13	-	-
17	15.41	-	-	-
18	15.98	1.10	0.63	1.73
19	16.42	1.88	0.67	2.55
20	14.81	0.29	0.20	0.49
21	16.24	-0.02	-0.05	-0.07
22	14.25	0.18	0.15	0.33
23	15.91	1.33	0.58	1.91
24	16.14	1.33	0.55	1.88
25	17.06	-	0.68	-
26	16.47	0.49	-	-
27	15.17	0.02	0.04	0.06
28	15.60	0.05	0.03	0.08
29	16.89	0.05	-	-
30	14.48	0.16	0.16	0.32
31	16.39	-	0.71	-
32	16.64	0.82	-	-
33	16.72	1.67	0.69	2.36
34	16.59	0.01	0.02	0.03
35	16.75	-	-0.02	-
36	16.75	0.45	-	-
37	15.59	1.26	0.71	1.97
38	15.69	1.15	0.76	1.91
39	16.24	0.09	-0.08	0.01
40	16.49	0.07	-	-
41	16.63	0.56	0.14	0.70
42	15.65	0.51	0.29	0.80
43	17.47	0.17	-0.02	0.15
44	16.56	0.09	0.05	0.14
45	16.49	-	0.17	-
46	16.26	-	-0.01	-
47	16.99	-0.06	0.01	-0.05
48	16.61	-	0.41	-
49	16.99	0.12	0.01	0.13
50	16.62	1.24	0.61	1.85
51	15.11	1.68	0.73	2.41
52	16.11	0.48	0.02	0.50
53	16.80	-	0.50	-
54	15.78	-0.08	0.11	0.03
55	16.17	1.67	0.71	2.38
56	15.96	0.97	-	-
57	15.45	1.39	0.63	2.02
58	16.50	1.21	0.58	1.79
59	16.16	-0.08	0.03	-0.05
60	16.10	-	0.11	-
61	16.58	-0.05	0.03	-0.02
62	16.50	-0.09	0.06	-0.03
63	13.76	-0.02	0.18	0.16
64	14.93	0.34	0.32	0.66
65	16.85	-0.01	-	-
66	15.73	1.17	0.64	1.81
67	16.19	-	-0.06	-
68	16.98	0.26	0.47	0.73
69	15.34	-0.15	0.12	-0.03
70	16.15	-	0.75	-
71	15.80	1.39	0.77	2.16
72	15.68	1.49	0.47	1.96
73	17.56	0.63	0.67	1.30
74	18.84	0.09	0.13	0.22
75	17.03	-0.07	0.19	0.12
76	18.64	0.67	0.43	1.10
77	18.53	0.05	-0.07	-0.02
78	18.19	-0.05	-0.01	-0.06
79	18.17	0.32	0.04	0.36
80	17.49	1.60	-	-
81	18.51	0.14	0.03	0.17
82	17.71	-	0.24	-
83	18.23	0.09	0.07	0.16

TABLE XVII. (continued)

Star	V	B-V	V-R	B-R
84	18.82	0.07	-	-
85	16.87	1.75	0.96	2.71
86	17.95	0.03	0.01	0.04
87	19.19	0.24	-	-
88	18.42	0.05	0.01	0.06
89	18.54	0.21	-	-
90	18.01	1.82	0.69	2.51
91	17.92	-	-0.02	-
92	18.53	0.22	-0.02	0.20
93	16.83	1.21	0.55	1.76
94	18.73	0.27	-	-
95	17.59	0.11	0.04	0.15
96	17.55	0.09	-	-
97	17.65	1.32	0.47	1.79
98	18.42	-	0.01	-
99	18.93	0.08	-0.03	0.05
100	17.69	0.15	-0.01	0.14
101	17.88	0.18	0.01	0.19
102	18.05	0.12	-0.01	0.11
103	18.33	0.67	-	-
104	18.38	0.06	-	-
105	17.71	0.32	-	-
106	17.87	0.89	0.30	1.19
107	17.61	1.48	0.70	2.18
108	18.42	-0.02	0.07	0.05
109	17.83	1.37	0.72	2.09
110	18.20	-0.03	0.08	0.05
111	18.99	0.05	0.16	0.21
112	18.86	-0.08	0.12	0.04
113	18.07	0.96	0.60	1.56
114	18.57	0.39	-	-
115	17.65	-0.03	0.02	-0.01
116	17.58	0.01	0.06	0.07
117	17.89	0.11	-	-
118	16.87	1.78	0.77	2.55
119	16.86	1.66	0.72	2.38
120	17.17	1.82	0.63	2.45
121	17.06	1.03	0.38	1.41
122	16.73	-0.04	0.02	-0.02
123	15.70	1.18	0.63	1.81
124	16.07	-	0.66	-
125	16.61	1.89	0.75	2.64
126	16.25	2.38	1.01	3.39
127	16.72	-	0.54	-
128	17.26	1.63	0.76	2.39
129	17.11	2.20	0.86	3.06
130	17.24	1.02	0.46	1.48
131	17.30	1.35	0.49	1.84
132	16.89	1.86	0.81	2.67
133	14.18	0.79	0.57	1.36
134	15.36	1.32	0.59	1.91
135	16.85	0.69	-	-
136	16.51	-	0.46	-
137	14.75	0.15	0.14	0.29
138	16.90	-	0.33	-
139	16.69	0.00	0.00	0.00
140	17.06	-	0.72	-
141	14.53	0.02	0.04	0.06
142	14.93	1.55	0.74	2.29
143	16.89	0.97	0.66	1.63
144	15.61	-0.11	0.06	-0.05
145	16.44	0.59	-	-
146	15.50	0.72	0.45	1.17
147	16.37	-	0.76	-
148	17.09	-	1.08	-
149	16.84	-	1.40	-
150	15.50	0.00	0.06	0.06
151	16.82	-	0.38	-
152	16.84	0.05	-	-
153	16.14	-	0.40	-
154	17.09	-	0.61	-
155	16.62	-	0.35	-
156	16.35	-	0.09	-
157	16.58	0.06	0.10	0.16
158	14.20	0.31	0.32	0.63
159	16.44	1.78	0.78	2.56
160	16.92	-	0.77	-
161	15.09	1.31	0.60	1.91
162	14.84	0.18	0.28	0.46
163	16.55	1.19	0.26	1.45
164	16.59	-	0.39	-
165	16.19	0.01	-	-
166	15.79	1.65	0.57	2.22
167	16.12	-0.08	-	-

TABLE XVII. (continued)

Star	V	B-V	V-R	B-R
168	15.55	0.50	0.32	0.82
169	16.30	0.19	0.16	0.35
170	14.39	0.56	0.27	0.83
171	15.34	0.70	0.21	0.91
172	15.53	1.74	0.78	2.52
173	15.38	0.64	0.21	0.85
174	16.46	0.10	0.07	0.17
175	16.54	1.17	0.30	1.47
176	15.33	-0.12	0.13	0.01
177	16.11	-	-	-
178	16.13	1.43	0.60	2.03
179	16.00	1.33	0.63	1.96
180	14.87	0.16	0.04	0.20
181	16.52	1.60	0.86	2.46
182	17.24	-	0.45	-
183	16.95	1.20	0.51	1.71
184	16.92	1.58	0.61	2.19
185	16.15	2.01	0.68	2.69
186	15.24	1.16	0.52	1.68
187	17.23	-	0.74	-
188	17.19	1.20	0.43	1.63
189	14.84	0.07	0.15	0.22
190	16.54	0.06	-	-
191	15.50	-0.09	0.06	-0.03
192	14.97	-0.07	-0.02	-0.09
193	16.29	-	0.06	-
194	16.87	2.21	0.69	2.90
195	15.88	0.07	-	-
196	14.76	0.41	-	-
197	16.63	0.12	0.11	0.23
198	17.71	0.05	-	-
199	17.41	1.36	0.57	1.93
200	18.52	0.05	-	-
201	18.93	0.11	-0.02	0.09
202	18.28	1.03	-	-
203	19.12	-0.06	0.13	0.07
204	19.14	0.20	0.17	0.37
205	18.97	0.28	0.15	0.43
206	18.36	0.18	-0.08	0.10
207	18.60	-	0.46	-
208	17.45	0.20	0.02	0.22
209	17.31	1.87	0.47	2.34
210	16.71	-	0.44	-
211	16.90	0.02	-0.01	0.01
212	17.94	1.25	0.55	1.80
213	18.87	0.04	0.01	0.05
214	17.59	1.23	0.50	1.73
215	18.81	1.82	-	-
216	18.12	-0.03	-	-
217	16.56	0.02	0.07	0.09
218	16.82	-0.05	0.02	-0.03
219	18.95	0.20	0.35	0.55
220	17.68	2.17	0.79	2.96
221	18.33	0.00	-	-
222	17.27	1.25	0.54	1.79
223	17.93	1.25	-	1.25
224	17.26	1.53	0.72	2.25
225	17.21	1.39	0.62	2.01
226	17.09	-0.04	0.04	0.00
227	18.27	0.09	-0.13	-0.04
228	18.23	0.15	-0.07	0.08
229	18.31	0.27	-0.03	0.24
230	18.38	0.00	0.00	0.00
231	16.21	0.12	0.06	0.18
232	16.85	0.19	0.08	0.27
233	16.66	1.87	0.77	2.64
234	16.82	1.76	0.83	2.59
235	16.73	0.07	0.08	0.15
236	17.61	0.13	-0.06	0.07
237	17.92	0.54	0.34	0.88
238	17.52	1.03	0.23	1.26
239	17.04	-0.04	0.16	0.12
240	16.99	0.22	0.02	0.24
241	15.95	1.44	0.74	2.18
242	17.00	2.02	-	-
243	16.51	1.79	0.74	2.53
244	16.91	0.13	-0.02	0.11
245	18.36	1.14	0.54	1.68
246	17.58	0.93	0.63	1.56
247	18.56	0.50	0.33	0.83
248	18.03	1.58	0.87	2.45
249	18.10	0.10	-	-
250	18.64	0.43	0.32	0.75
251	18.79	0.29	-	-

TABLE XVIII. Photographic magnitudes and colors in NGC 1854.

Star	V	V-I	R-I	B-I	Star	V	V-I	R-I	B-I
2	14.91	0.75	-	2.06	63	13.76	0.36	0.18	0.34
3	14.37	0.54	-	0.89	64	14.93	0.55	0.23	0.89
4	14.00	0.06	-	-0.13	66	15.73	1.33	0.69	2.50
5	14.58	0.50	-	0.68	70	16.15	1.70	0.95	-
6	15.07	1.18	-	1.94	71	15.80	1.45	0.68	2.84
7	14.72	0.35	-	0.56	123	15.70	1.39	0.76	2.57
8	15.67	1.29	0.54	-	133	14.18	0.94	0.37	1.73
9	15.38	1.40	0.62	2.68	134	15.36	1.33	0.74	2.65
10	13.75	0.82	-	-	137	14.75	0.33	0.19	0.48
11	14.37	1.60	-	-	141	14.53	0.17	0.13	0.19
12	15.15	1.06	-	1.86	142	14.93	1.58	0.84	3.13
13	15.24	1.17	-	1.33	147	16.37	1.86	1.10	-
14	14.25	0.52	-	-	158	14.20	0.57	0.25	0.88
17	15.41	1.52	-	-	160	16.92	2.54	1.77	-
18	15.98	1.29	0.66	2.39	161	15.09	1.31	0.71	2.62
20	14.81	0.55	0.35	0.84	162	14.84	0.51	0.23	0.69
22	14.25	0.36	0.21	0.54	166	15.79	1.32	0.75	2.97
30	14.48	0.43	0.27	0.59	170	14.39	0.65	0.38	1.21
31	16.39	2.04	1.33	-	172	15.53	2.09	1.31	3.83
37	15.59	1.31	0.60	2.57	173	15.38	0.99	0.78	1.63
38	15.69	1.39	0.63	2.54	177	16.11	1.59	-	-
51	15.11	1.57	0.84	3.25	185	16.15	1.68	1.00	3.69
55	16.17	1.70	0.99	3.37	186	15.24	1.11	0.59	2.27
57	15.45	1.40	0.77	2.79	189	14.84	0.39	0.24	0.46

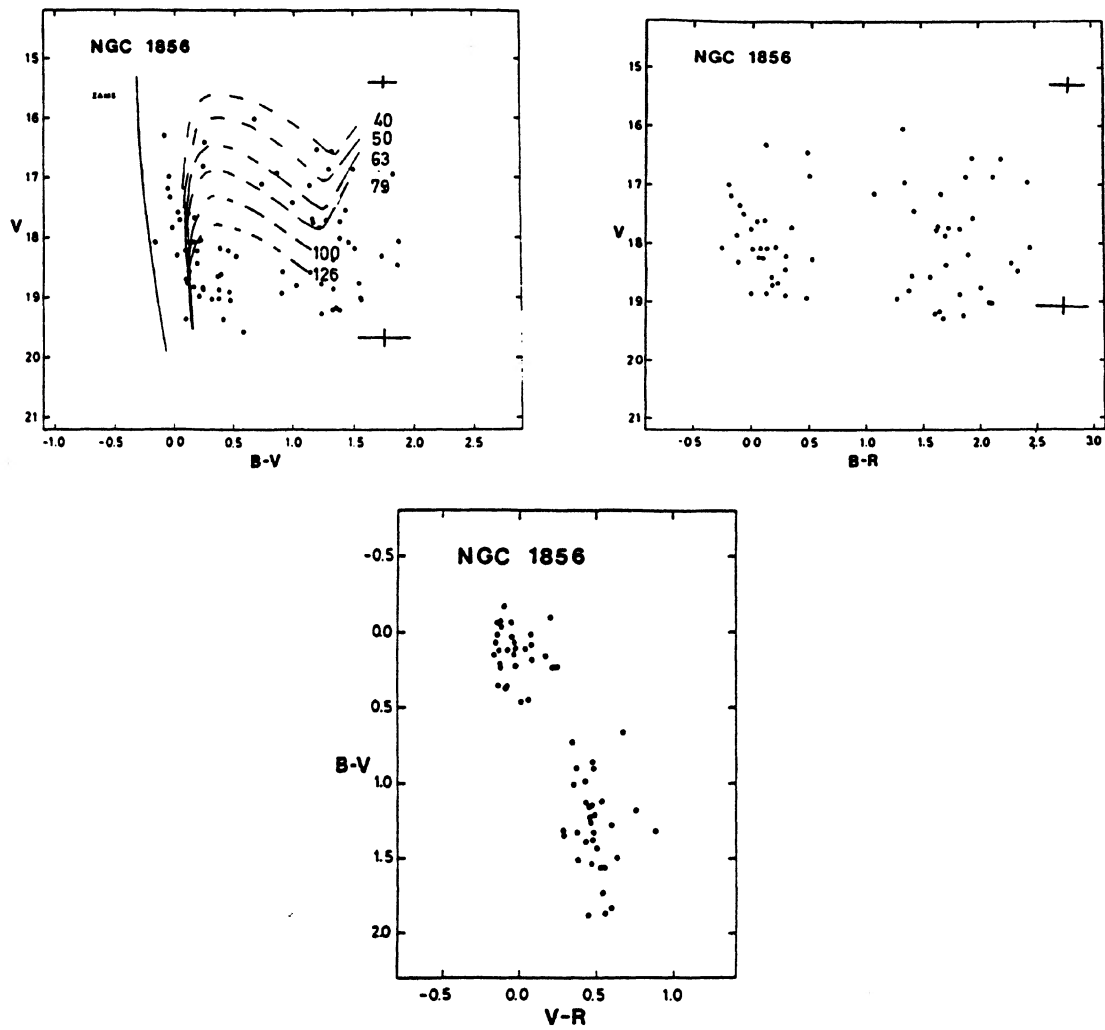


FIG. 21. Color-magnitude diagrams and color-color diagram of NGC 1856.

TABLE XIX. Photographic magnitudes and colors in NGC 1856.

Star	V	B-V	V-R	B-R	Star	V	B-V	V-R	B-R
1	17.60	0.12	-0.08	0.04	53	17.38	-	0.55	-
2	19.03	0.37	-	-	54	18.59	-	-0.14	-
3	16.81	0.24	0.25	0.49	55	18.87	1.33	0.48	1.81
4	18.83	0.16	-0.17	-0.01	56	17.55	1.44	0.50	1.94
5	19.37	0.09	-	-	57	18.88	0.37	-0.08	0.29
6	16.99	-0.05	-0.15	-0.20	58	18.07	1.88	0.55	2.43
7	18.09	0.14	-0.14	0.00	59	17.12	0.73	0.35	1.08
8	19.02	-	-0.10	-	60	18.43	0.19	0.09	0.28
9	18.07	0.15	-0.02	0.13	61	18.76	-	0.28	-
10	18.14	-	0.28	-	62	19.05	0.32	-	-
11	16.86	1.29	0.59	1.88	63	17.58	0.03	0.07	0.10
12	16.16	-	0.58	-	64	18.83	0.24	-0.12	0.12
13	17.20	-	0.39	-	65	18.65	-	-0.15	-
14	17.19	-0.06	-0.13	-0.19	66	16.87	1.50	0.62	2.12
15	18.61	-	0.08	-	67	18.58	1.13	0.43	1.56
16	18.42	-	0.00	-	68	17.83	1.21	0.49	1.70
17	17.70	1.15	0.48	1.63	69	19.59	0.58	-	-
18	17.84	-0.02	-0.12	-0.14	70	18.57	0.12	0.04	0.16
19	18.01	-	-0.28	-	71	19.22	1.38	0.47	1.85
20	18.70	0.09	0.08	0.17	72	19.06	0.47	-	-
21	18.33	-	0.04	-	73	18.19	1.51	0.38	1.89
22	18.78	0.10	-	-	74	18.57	0.91	0.49	1.40
23	16.30	-0.09	0.20	0.11	75	17.28	-	-0.01	-
24	17.42	0.99	0.43	1.42	76	18.24	0.11	-0.02	0.09
25	18.77	1.54	0.46	2.00	77	18.17	-	0.40	-
26	17.96	-	-0.05	-	78	17.71	1.26	0.46	1.72
27	18.22	0.08	-0.03	0.05	79	16.33	-	-0.05	-
28	16.93	0.86	0.49	1.35	80	16.53	1.19	0.75	1.94
29	19.38	0.41	-	-	81	16.02	0.67	0.67	1.34
30	18.32	1.74	0.53	2.27	82	19.31	-	0.51	-
31	18.30	0.02	-0.15	-0.13	83	19.11	-	0.04	-
32	18.93	0.90	0.37	1.27	84	19.17	1.35	0.29	1.64
33	17.49	0.08	-0.15	-0.07	85	18.80	1.03	0.35	1.38
34	18.62	0.39	-	-	86	18.99	0.21	-	-
35	17.95	-	0.42	-	87	18.40	0.12	-	-
36	18.08	-0.16	-0.10	-0.26	88	18.15	-	0.38	-
37	17.34	-0.05	-0.05	-0.10	89	16.56	1.32	0.88	2.20
38	16.95	1.84	0.59	2.43	90	16.42	0.24	0.23	0.47
39	17.74	1.39	0.43	1.82	91	17.76	1.16	0.45	1.61
40	17.13	1.13	0.53	1.66	92	19.01	1.56	0.52	2.08
41	17.73	0.04	-0.05	-0.01	93	18.69	-	0.44	-
42	18.78	1.22	-	-	94	19.28	-	0.67	-
43	18.37	1.33	0.37	1.70	95	18.92	0.46	0.01	0.47
44	18.66	0.36	-0.14	0.22	96	19.28	1.23	0.45	1.68
45	18.24	0.19	-	-	97	17.70	0.16	0.17	0.33
46	18.17	-	0.18	-	98	18.19	0.38	-0.09	0.29
47	18.05	0.22	-0.02	0.20	99	17.74	-	-0.54	-
48	18.05	0.21	-0.13	0.08	100	19.02	1.56	0.54	2.10
49	19.21	1.32	0.28	1.60	101	18.32	0.51	-	-
50	18.47	1.88	0.44	2.32	102	18.88	0.24	-	-
51	17.09	-	0.59	-	103	18.01	1.39	-	-
52	18.23	0.45	0.06	0.51	104	18.08	1.46	-	-

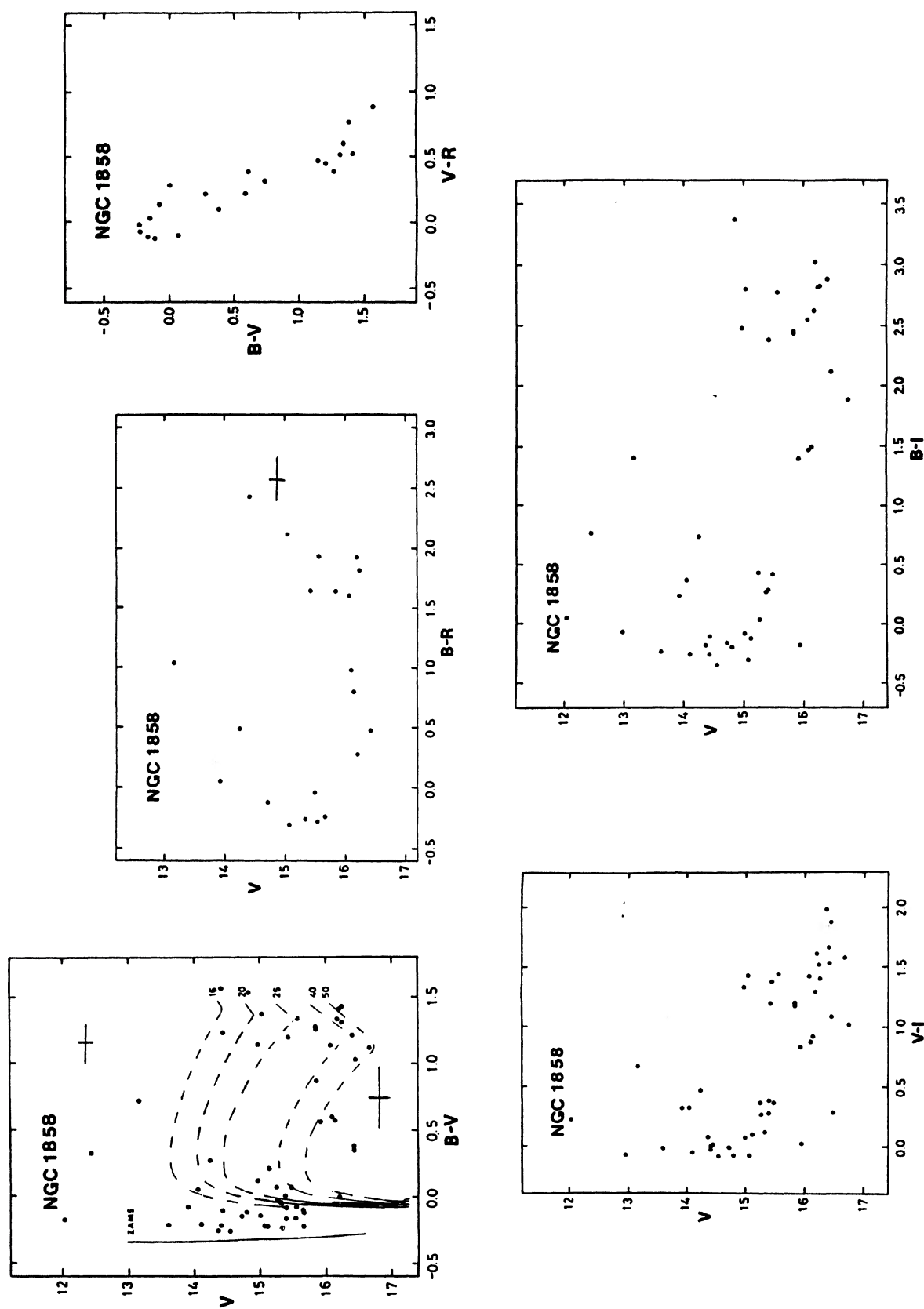


FIG. 23. Color-magnitude diagrams and color-color diagram of NGC 1858.

TABLE XX. Photographic magnitudes and colors in NGC 1858.

Star	V	B-V	V-R	B-R
1	16.48	-	0.26	-
2	15.32	-0.05	-	-
3	16.20	1.41	0.52	1.93
4	16.08	1.14	0.47	1.61
5	15.40	-0.17	-	-
6	16.26	1.43	-	-
7	15.25	0.07	-	-
8	15.57	1.34	0.60	1.94
9	17.59	-	1.30	-
10	13.91	-0.08	0.13	0.05
11	16.40	1.22	-	-
12	14.05	0.05	-	-
13	15.42	1.20	0.45	1.65
14	15.66	-0.11	-0.13	-0.24
15	16.36	-	-	-
16	16.41	-	0.39	-
17	14.83	1.53	-	-
18	15.39	0.00	-	-
19	15.40	-0.09	-	-
20	15.27	-0.03	-	-
21	15.44	-	-	-
22	16.10	0.60	0.39	0.99
23	14.97	0.12	-	-
24	16.20	0.00	0.28	0.28
25	16.42	0.35	-	-
26	14.24	0.27	0.22	0.49
27	15.91	0.56	-	-
28	14.10	-0.21	-	-
29	14.42	-0.11	-	-
30	12.43	0.32	-	-
31	15.66	-0.23	-	-
32	15.56	-0.08	-	-
33	14.36	-0.26	-	-
34	15.00	-0.15	-	-
35	16.44	-	-	-
36	16.66	1.12	-	-
37	15.14	0.21	-	-
38	14.41	-0.22	-	-
39	15.78	-	0.36	-
40	14.71	-0.15	0.03	-0.12
41	17.01	-	0.33	-
42	14.53	-0.26	-	-
43	15.11	-0.23	-	-
44	13.60	-0.21	-	-
45	14.80	-0.12	-	-
46	15.33	-0.24	-0.02	-0.26
47	13.16	0.73	0.31	1.04
48	15.84	1.27	-	-
49	15.84	1.26	0.39	1.65
50	16.19	1.34	-	-
51	16.13	0.58	0.22	0.80
52	15.49	0.06	-0.10	-0.04
53	15.65	-0.12	-	-
54	15.07	-0.23	-0.07	-0.30
55	15.04	1.37	0.76	2.13
56	16.41	0.38	0.10	0.48
57	14.41	1.56	0.88	2.44
58	14.98	1.14	-	-
59	15.86	0.88	-	-
60	15.53	-0.17	-0.11	-0.28
61	12.01	-0.18	-	-
62	16.67	-	0.23	-
63	16.45	1.03	-	-
64	16.24	1.31	0.51	1.82

TABLE XXI. Photographic magnitudes and colors in NGC 1858.

Star	V	V-I	R-I	B-I	Star	V	V-I	R-I	B-I
1	16.48	0.28	0.02	-	34	15.00	0.06	-	-0.09
2	15.32	0.11	-	-	35	16.44	1.88	-	-
3	16.20	1.61	1.09	3.02	37	15.93	0.03	-	-0.18
4	16.08	1.41	0.94	2.55	38	14.41	-0.04	-	-0.26
6	16.26	1.40	-	2.83	40	14.71	-0.01	-0.04	-0.16
7	15.25	0.36	-	0.43	42	14.53	-0.09	-	-0.35
8	15.57	1.44	0.84	2.78	43	15.11	0.10	-	-0.13
10	13.91	0.32	0.19	0.24	44	13.60	-0.03	-0.41	-0.24
11	16.40	1.66	1.43	2.88	45	14.80	-0.08	-	-0.20
12	14.05	0.32	-	0.37	47	13.16	0.67	0.36	1.40
13	15.42	1.19	0.74	2.39	48	15.84	1.17	-	2.44
15	16.36	1.99	-	-	49	15.84	1.19	0.80	2.45
16	16.41	1.53	1.14	-	50	16.19	1.29	1.08	2.63
18	15.39	0.27	-	0.27	51	16.13	0.92	0.70	1.50
19	15.40	0.37	-	0.28	52	15.49	0.36	0.46	0.42
20	15.27	0.26	-	0.03	54	15.07	-0.08	-0.01	-0.31
21	15.44	1.38	-	-	55	15.04	1.43	0.67	2.80
22	16.10	0.87	0.48	1.47	58	14.98	1.33	-	2.47
26	14.24	0.47	0.25	0.74	59	16.74	1.01	-	1.89
27	15.91	0.84	-	1.40	61	12.01	0.23	-	0.05
28	14.10	-0.05	-	-0.26	62	16.67	1.58	1.35	-
29	14.42	0.00	-	-0.11	63	16.45	1.09	1.08	2.12
30	12.43	0.44	-	0.76	64	16.24	1.51	1.00	2.82
33	14.36	0.07	-	-0.19					

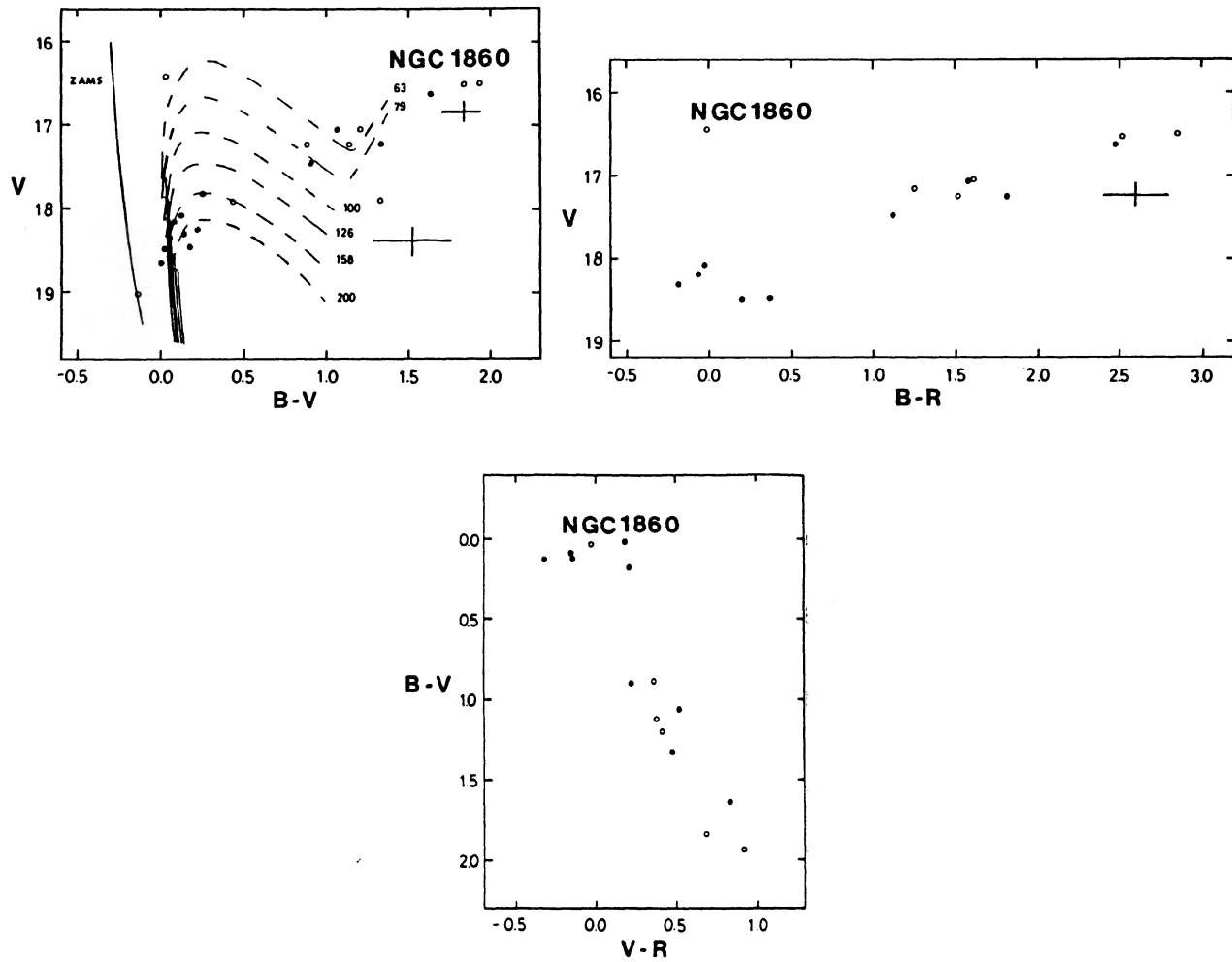


FIG. 25. Color-magnitude diagrams and color-color diagram of NGC 1860.

TABLE XXII. Photographic magnitudes and colors in NGC 1860.

Star	V	B-V	V-R	B-R
1	18.30	0.14	-0.33	-0.19
2	18.25	0.21	-	-
3	18.49	0.02	0.18	0.20
4	16.62	1.64	0.83	2.47
5	18.09	0.12	-0.15	-0.03
6	17.48	0.90	0.22	1.12
7	18.46	0.17	0.20	0.37
8	18.19	0.09	-0.16	-0.07
9	17.06	1.06	0.52	1.58
10	17.82	0.25	-	-
11	17.24	1.33	0.48	1.81
12	18.64	0.00	-	-
13	18.99	-	1.33	-
14	19.01	-0.14	-	-
15	17.13	0.89	0.36	1.25
16	17.91	0.44	-	-
17	17.23	1.13	0.38	1.51
18	16.42	0.03	-0.04	-0.01
19	17.04	1.20	0.41	1.61
20	16.54	-	0.48	-
21	17.90	1.33	-	-
22	16.51	1.84	0.68	2.52
23	16.50	1.94	0.91	2.85

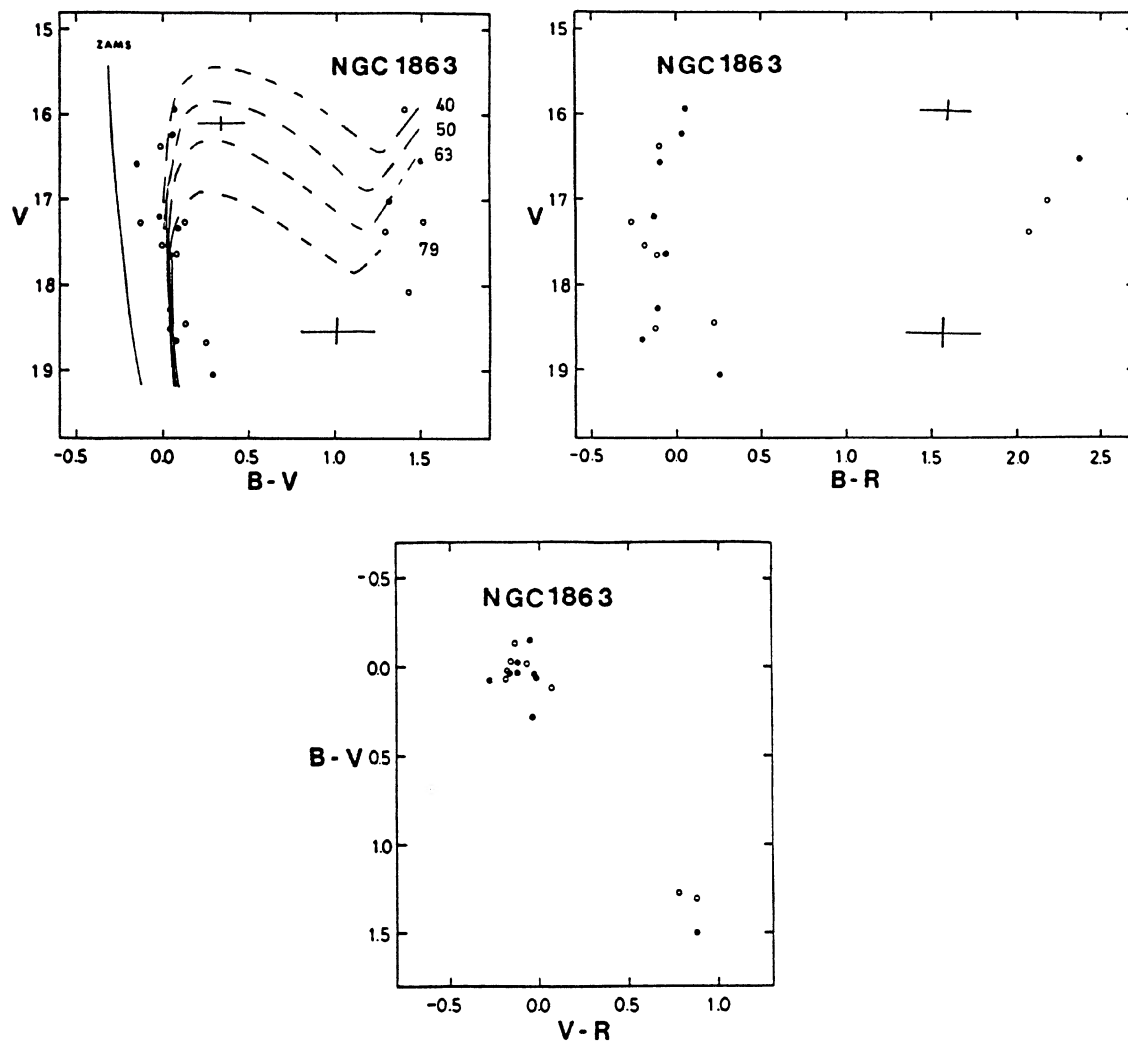


FIG. 27. Color-magnitude diagrams and color-color diagram of NGC 1863.

TABLE XXIII. Photographic magnitudes and colors in NGC 1863.

Star	V	B-V	V-R	B-R
1	17.34	0.09	-	-
2	17.63	0.04	-0.11	-0.07
3	15.93	0.06	-0.01	0.05
4	16.22	0.05	-0.03	0.02
5	16.59	-0.15	0.05	-0.10
6	18.63	0.08	-0.29	-0.21
7	16.53	1.50	0.87	2.37
8	19.05	0.28	-0.03	0.25
9	17.20	-0.02	-0.12	-0.14
10	18.29	0.04	-0.16	-0.12
11	17.01	1.31	0.87	2.18
12	17.63	0.07	-0.19	-0.12
13	15.94	1.40	-	-
14	17.53	-0.03	-0.16	-0.19
15	18.45	0.13	0.08	0.21
16	17.39	1.29	0.77	2.06
17	18.07	1.42	-	-
18	16.39	-0.02	-0.08	-0.10
19	17.27	0.12	-	-
20	18.51	0.03	-0.16	-0.13
21	17.18	-0.14	-0.13	-0.27
22	18.69	0.25	-	-
23	17.26	1.51	-	-

TABLE XXIV. Photographic magnitudes and colors in NGC 1870.

Star	V	B-V	V-R	B-R
1	14.95	0.20	-	-
2	16.25	-0.21	-	-
3	16.75	-0.13	-	-
4	14.95	0.24	0.22	0.46
5	17.48	0.93	-	-
6	18.42	-0.01	-	-
7	16.39	0.12	-	-
8	18.40	0.12	-	-
9	17.14	1.93	-	-
10	16.91	0.24	-	-
11	18.29	-0.26	-	-
12	17.53	1.56	-	-
13	17.34	-0.09	-	-
14	18.63	0.01	-	-
15	18.11	0.19	-	-
16	18.26	0.13	-	-
17	17.01	0.52	-	-
18	17.84	-0.09	-	-
19	18.39	0.07	-	-
20	15.35	1.47	0.84	2.31
21	16.65	0.30	-	-
22	18.54	0.09	-	-

SL 234 (Figs. 30 [Plate 47] and 31; Table XXV). Of the 16 stars measured, four are found in the forbidden rectangle.

SL 237 (Figs. 32 [Plate 48] and 33; Tables XXVI and XXVII). This seems to be a young cluster on the basis of the several bright stars ( $V < 14$ ).

SL 304 (Figs. 34 [Plate 49] and 35; Table XXVIII). The five stars in the forbidden rectangle appear to lie along an isochrone at  $30 \times 10^6$  yr.

##### V. CONCLUSIONS

The clusters studied here are all significantly younger than the stars in the general field of the bar of the LMC (Hardy *et al.* 1984), but not as young as the youngest galac-

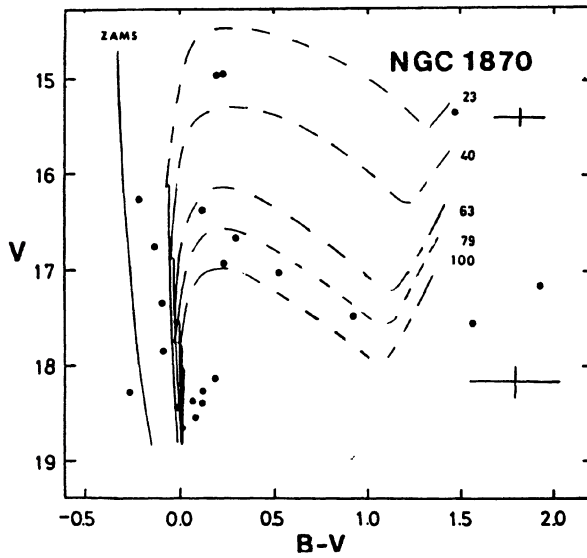
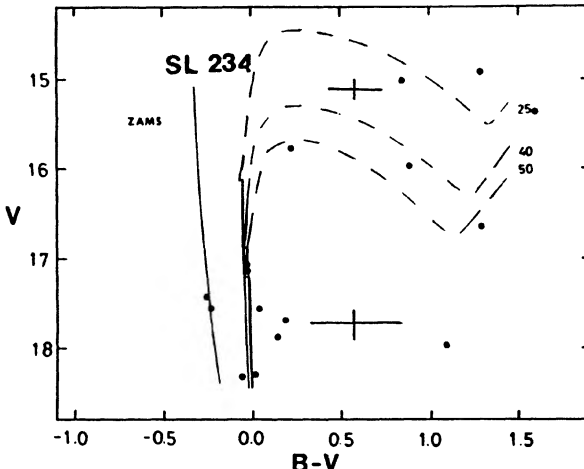
FIG. 29.  $V$  vs  $B - V$  color-magnitude diagram of NGC 1870.FIG. 31.  $V$  vs  $B - V$  color-magnitude diagram of SL 234.

TABLE XXV. Photographic magnitudes and colors in SL 234.

Star	V	B-V	V-R	B-R
1	15.78	0.22	-	-
2	17.96	1.09	-	-
3	18.29	0.01	-	-
4	15.98	0.89	0.45	1.34
5	17.79	0.18	-	-
6	17.54	0.04	-	-
7	15.36	1.58	0.75	2.33
8	17.88	0.14	-	-
9	17.14	-0.02	-	-
10	15.01	0.85	-	-
11	17.41	-0.26	-	-
12	17.56	-0.24	-	-
13	18.31	-0.06	-	-
14	16.63	1.29	-	-
15	14.93	1.29	0.64	1.93
16	17.06	-0.04	-	-

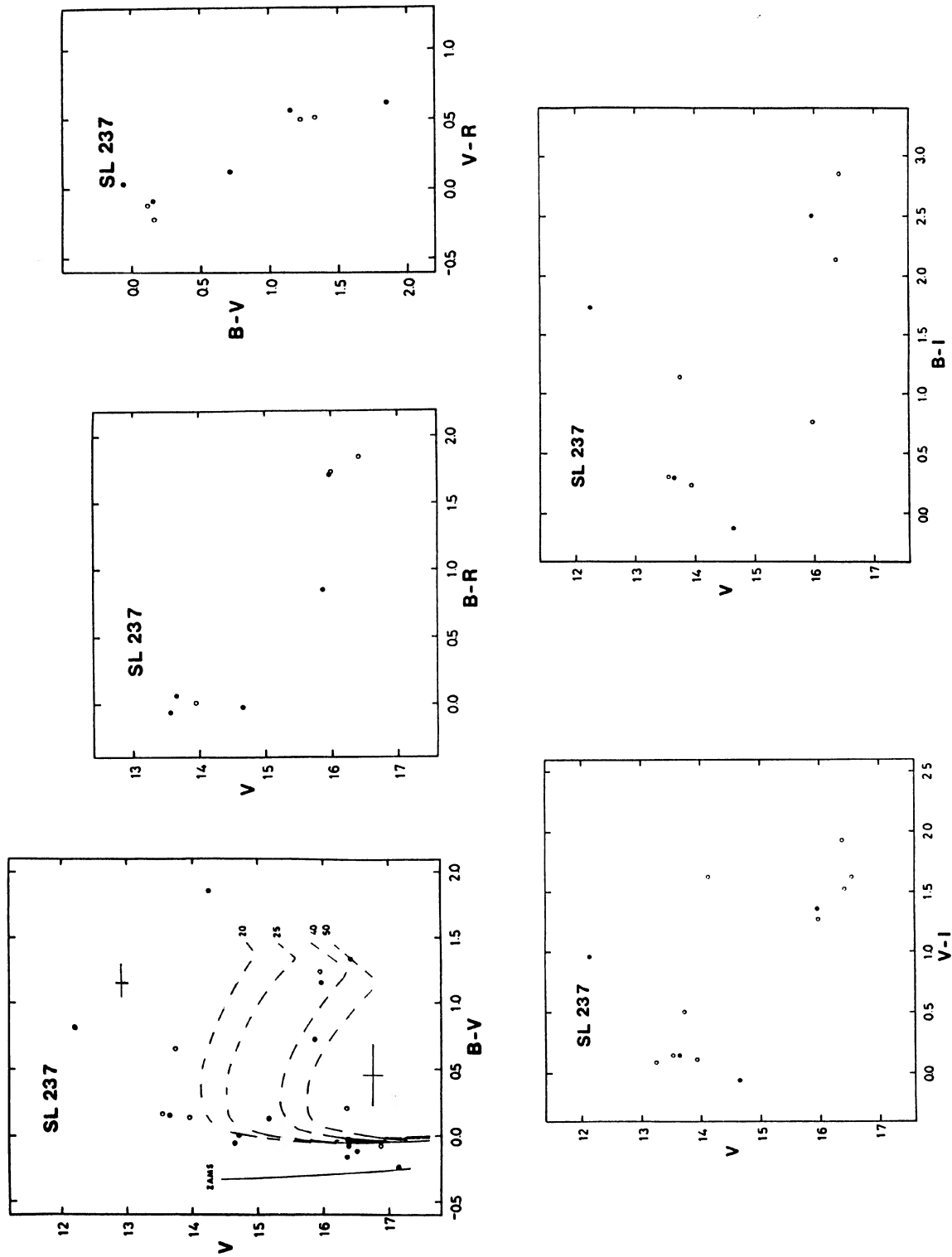


FIG. 33. Color-magnitude diagrams and color-color diagram of SL 237.

TABLE XXVI. Photographic magnitudes and colors in SL 237.

Star	V	B-V	V-R	B-R
1	12.23	0.78	-	0.85
2	15.88	0.72	0.13	0.56
3	15.97	1.15	0.56	1.71
4	17.13	-0.24	-	-
5	16.51	-0.12	-	-
6	16.38	-0.03	-	-
7	13.64	0.15	-0.09	0.06
8	16.38	-0.16	-	-
9	14.70	0.00	-	-
10	16.39	-0.08	-	-
11	16.40	-	0.05	-
12	16.01	-	0.29	-
13	14.26	1.85	0.63	2.48
14	14.63	-0.06	0.04	-0.02
15	15.18	0.12	-	-
16	14.13	-	0.59	-
17	16.42	1.33	0.51	1.84
18	13.73	0.65	-	-
19	13.25	-	0.02	-
20	13.54	0.16	-0.22	-0.06
21	16.53	-	0.49	-
22	13.94	0.13	-0.12	0.01
23	16.38	0.20	-	-
24	15.98	1.23	0.50	1.73
25	16.88	-0.08	-	-

TABLE XXVII. Photographic magnitudes and colors in SL 237.

Star	V	B-I	V-I	R-I	B-I
1	12.23	-	0.96	-	1.74
3	15.97	0.13	1.36	0.80	2.51
7	16.39	15.97	13.64	0.15	0.30
14	16.40	-	14.63	-0.06	-0.12
16	16.01	-	14.13	1.63	1.04
17	14.26	0.63	16.42	1.53	1.02
18	14.63	0.04	13.73	0.50	0.48
19	15.18	-	13.25	0.09	0.07
20	14.13	0.59	19	-	-
21	16.42	0.51	20	13.54	0.15
22	13.73	-	21	16.53	1.63
23	13.25	-	22	13.94	1.14
24	13.54	0.16	23	16.38	0.11
25	16.53	-	24	15.98	0.33
		-			0.24
		-			1.20
		-			2.14
		-			2.50

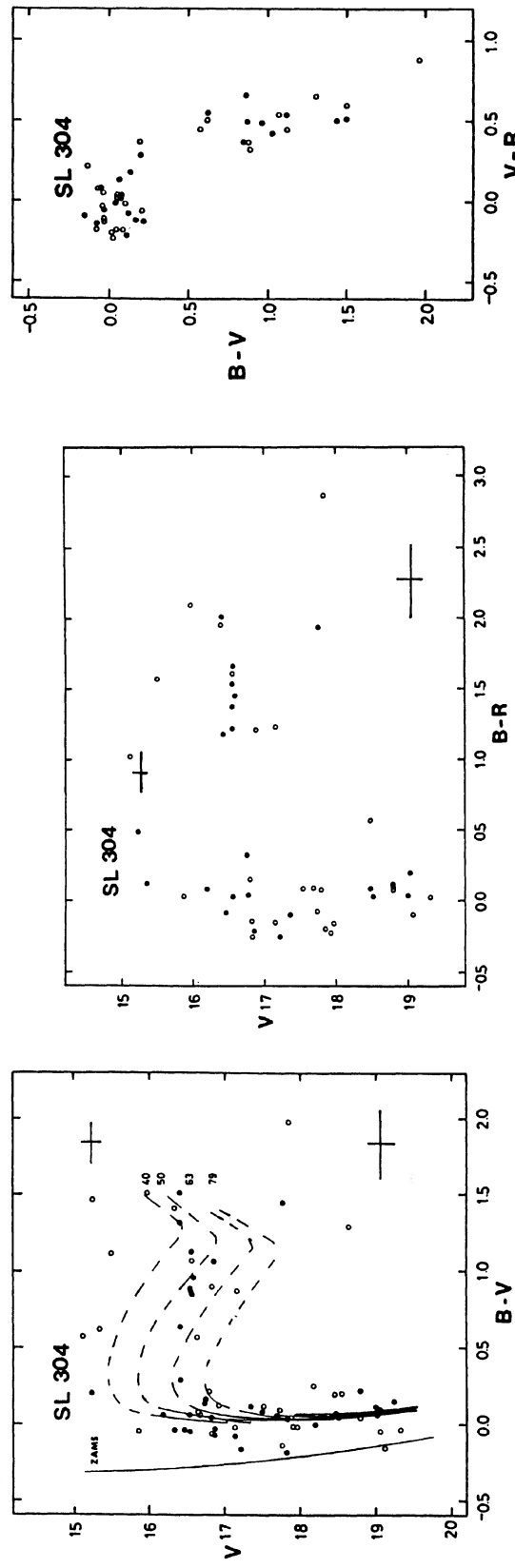


FIG. 35. Color-magnitude diagrams and color-color diagram of SL 304.

TABLE XXVIII. Photographic magnitudes and colors in SL 304.

Star	V	B-V	V-R	B-R
1	16.73	0.14	0.18	0.32
2	16.75	0.16	-0.12	0.04
3	16.40	0.63	0.55	1.18
4	16.55	1.12	0.54	1.66
5	16.53	0.06	-	-
6	16.40	1.50	0.51	2.01
7	16.41	0.28	-	-
8	16.67	-	0.71	-
9	16.59	0.96	0.49	1.45
10	16.84	-	0.37	-
11	16.63	-	0.45	-
12	16.55	0.87	0.66	1.53
13	16.54	-	0.81	-
14	16.33	-0.04	-	-
15	17.50	0.08	-	-
16	16.55	0.87	0.50	1.37
17	16.83	1.03	0.42	-
18	16.88	-0.04	-	-
19	17.14	-0.08	-	-
20	17.21	-0.16	-0.09	-0.25
21	18.51	0.04	-0.01	0.03
22	15.22	0.20	0.29	0.49
23	17.76	1.44	0.50	1.94
24	19.02	0.06	0.14	0.20
25	19.06	0.10	-	-
26	16.45	-0.04	-0.05	-0.09
27	18.20	0.00	-	-
28	19.24	0.15	-	-
29	16.84	-0.07	-0.14	-0.21
30	17.35	0.11	-0.21	-0.10
31	17.81	-0.19	-	-
32	19.12	-	-0.01	-
33	19.00	0.12	-0.08	0.04
34	18.48	0.07	0.01	0.08
35	18.80	0.22	-0.12	0.10
36	16.53	-0.05	0.08	0.03
37	16.54	0.85	0.37	1.22
38	16.19	0.06	0.02	0.08
39	18.79	0.06	0.04	0.10
40	18.36	-	0.29	-
41	18.64	1.29	-	-
42	19.41	-	0.14	-
43	16.31	1.41	-	-
44	16.91	0.12	-	-
45	16.74	-	0.60	-
46	16.77	-	0.56	-
47	16.77	-	0.59	-
48	15.32	0.62	0.50	1.12
49	16.57	1.06	0.54	1.60
50	16.75	-	0.74	-
51	18.16	0.25	-	-
52	18.47	0.19	0.37	0.56
53	17.77	-0.14	0.22	0.08
54	17.97	-0.02	-0.14	-0.16
55	18.79	0.07	0.01	0.08
56	19.33	-0.03	0.05	0.02
57	18.54	0.20	-	-
58	17.73	0.09	-0.17	-0.08
59	17.52	0.11	-0.02	0.09
60	15.11	0.57	0.45	1.02
61	19.13	-0.16	-	-
62	16.79	0.21	-0.06	0.15
63	16.83	0.89	0.32	1.21
64	16.82	0.04	-0.18	-0.14
65	15.97	1.50	0.60	2.10
66	17.84	1.97	0.89	2.86
67	17.69	0.05	0.04	0.09
68	18.87	-	0.00	-
69	19.06	-0.04	-0.05	-0.09
70	16.82	-0.07	-0.18	-0.25
71	16.64	0.57	-	-
72	16.40	1.31	0.65	1.96
73	15.49	1.12	0.45	1.57
74	16.67	0.06	-	-
75	15.25	1.47	-	-
76	15.86	-0.05	0.08	0.03
77	16.66	0.06	-	-
78	17.15	-0.02	-0.13	-0.15
79	17.84	0.03	-0.23	-0.20
80	17.92	-0.02	-0.20	-0.22
81	17.16	0.87	0.37	1.24

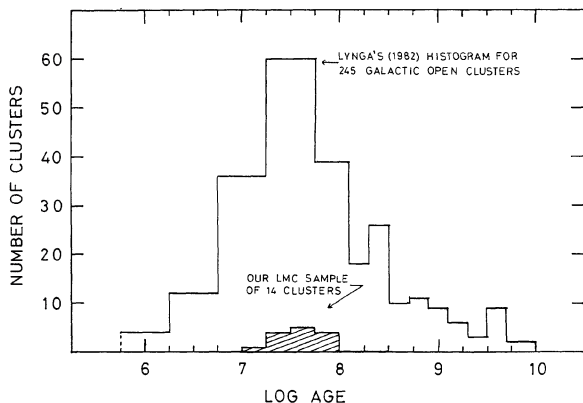


FIG. 36. Lyngå's (1982) histogram of galactic cluster ages together with the 14 clusters studied here.

tic clusters found so far, such as NGC 2264, NGC 6231, and Orion (Mermilliod 1981; Tarrab 1982).

We find a significant number of stars lying in a region not frequently occupied by LMC bar stars. In the absence of any other explanation, we have assumed in the discussion of the individual clusters that they are rapidly evolving stars that, for some reason, appear in substantial number in the clusters studied here.

In a summary of his *Catalogue of Galactic Clusters*, Lyngå (1982) has included ages for 245 objects from 47 different references. These ages range approximately from  $10^6$  yr to almost  $10^{10}$  yr. Figure 36 shows Lyngå's (1982) histogram of galactic cluster age together with the 14 clusters studied here. It is seen that our sample of LMC clusters is located quite close to the center of the histogram with the same, roughly Gaussian distribution. Both groups peak at  $\log_{10} \text{age} \sim 7.5$ .

It is a pleasure to thank the ESO, Las Campanas, and Cerro Tololo observing programs committees for allocating telescope time for this project. Thanks are due to Franklin Alvarado and Isabel Ormeño, research assistants at the Isaac Newton Institute, for their contribution in the data reduction.

#### REFERENCES

- Alcaino, G., and Liller, W. (1982). *Astron. Astrophys.* **114**, 213.
- Allen, C. W. (1973). *Astrophysical Quantities*, third ed. (Athlone, London).
- Becker, S. A., and Mathews, G. J. (1983). *Astrophys. J.* **270**, 155.
- Bok, J. B., and Bok, P. F. (1969). *Astron. J.* **74**, 1125.
- Brunish, W. (1981). Ph. D. thesis, University of Illinois.
- Carney, B. W., Janes, K. A., and Flower, P. J. (1985). *Astron. J.* **90**, 1196.
- Connolly, L. P., and Tifft, W. G. (1977). *Mon. Not. R. Astron. Soc.* **180**, 401.
- Durand, D., Hardy, E., and Melnick, J. (1984). *Astrophys. J.* **283**, 552.
- Hardy, E., Buonanno, R., Corsi, C., Jones, K., and Schommer, R. A. (1984). *Astrophys. J.* **278**, 592.
- Hodge, P. W. (1983). *Astrophys. J.* **264**, 470.
- Hodge, P. W., and Lee, S. O. (1984). *Astrophys. J.* **276**, 509.
- Lyngå, G. (1982). *Astron. Astrophys.* **109**, 213.
- Maeder, A., and Mermilliod, J. C. (1981). *Astron. Astrophys.* **93**, 136.
- Nelson, M., and Hodge, P. W. (1983). *Publ. Astron. Soc. Pac.* **95**, 5.
- Olszewski, E. W. (1984). *Astrophys. J.* **284**, 108.
- Robertson, J. W. (1974). *Astron. Astrophys. Suppl.* **15**, 261.
- Sandage, A. R. (1982). *Astrophys. J.* **252**, 553.
- Sandage, A. R., and Tammann, G. (1974). *Astrophys. J.* **190**, 525.
- Schlesinger, B. (1969). *Astrophys. J.* **157**, 533.
- Schommer, R. A., Olszewski, E. W., and Aaronson, M. (1984). *Astrophys. J. Lett.* **285**, L53.
- Stothers, R. (1972). *Astrophys. J.* **175**, 431.
- Stryker, L. L. (1983). *Astrophys. J.* **266**, 82.
- Tarrab, I. (1982). *Astron. Astrophys.* **113**, 57.
- Taylor, B. J. (1986). *Astrophys. J. Suppl.* **60**, 577.
- Tifft, W. G., and Connolly, L. P. (1973). *Mon. Not. R. Astron. Soc.* **163**, 93.
- Tifft, W. G., and Snell, Ch. M. (1971). *Mon. Not. R. Astron. Soc.* **151**, 365.
- VandenBerg, D. A. (1985). *Astrophys. J. Suppl.* **58**, 711.
- van den Bergh, S. (1981). *Astron. Astrophys. Suppl.* **46**, 79.
- van den Bergh, S., and Boer, K. S. (1984). In *Structure and Evolution of the Magellanic Clouds*, edited by S. van den Bergh and K. S. de Boer (Reidel, Dordrecht), p. 49.

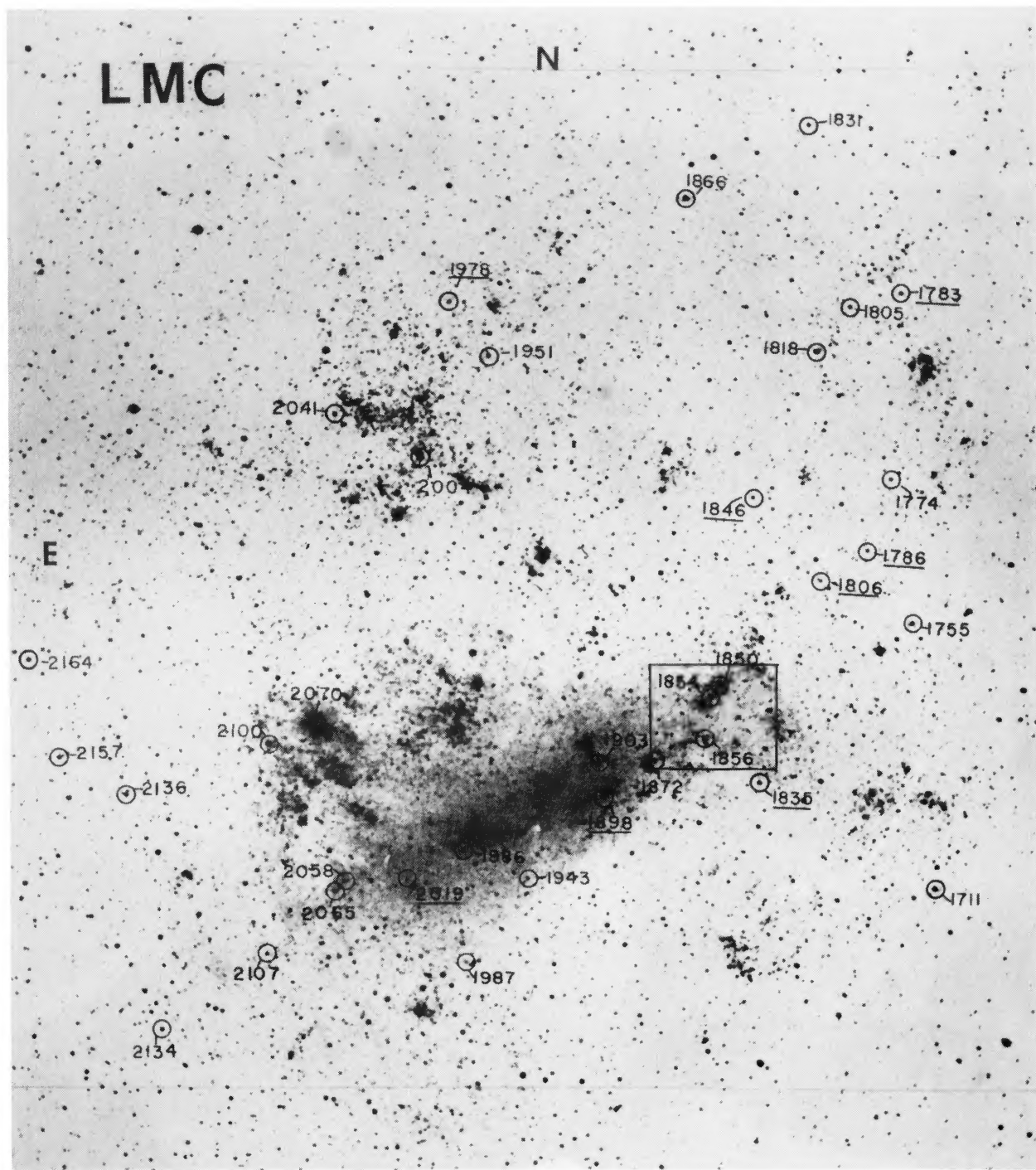


FIG. 1. The Large Magellanic Cloud. The studied Bok region is circumscribed in a square.

G. Alcaino and W. Liller (see page 372)

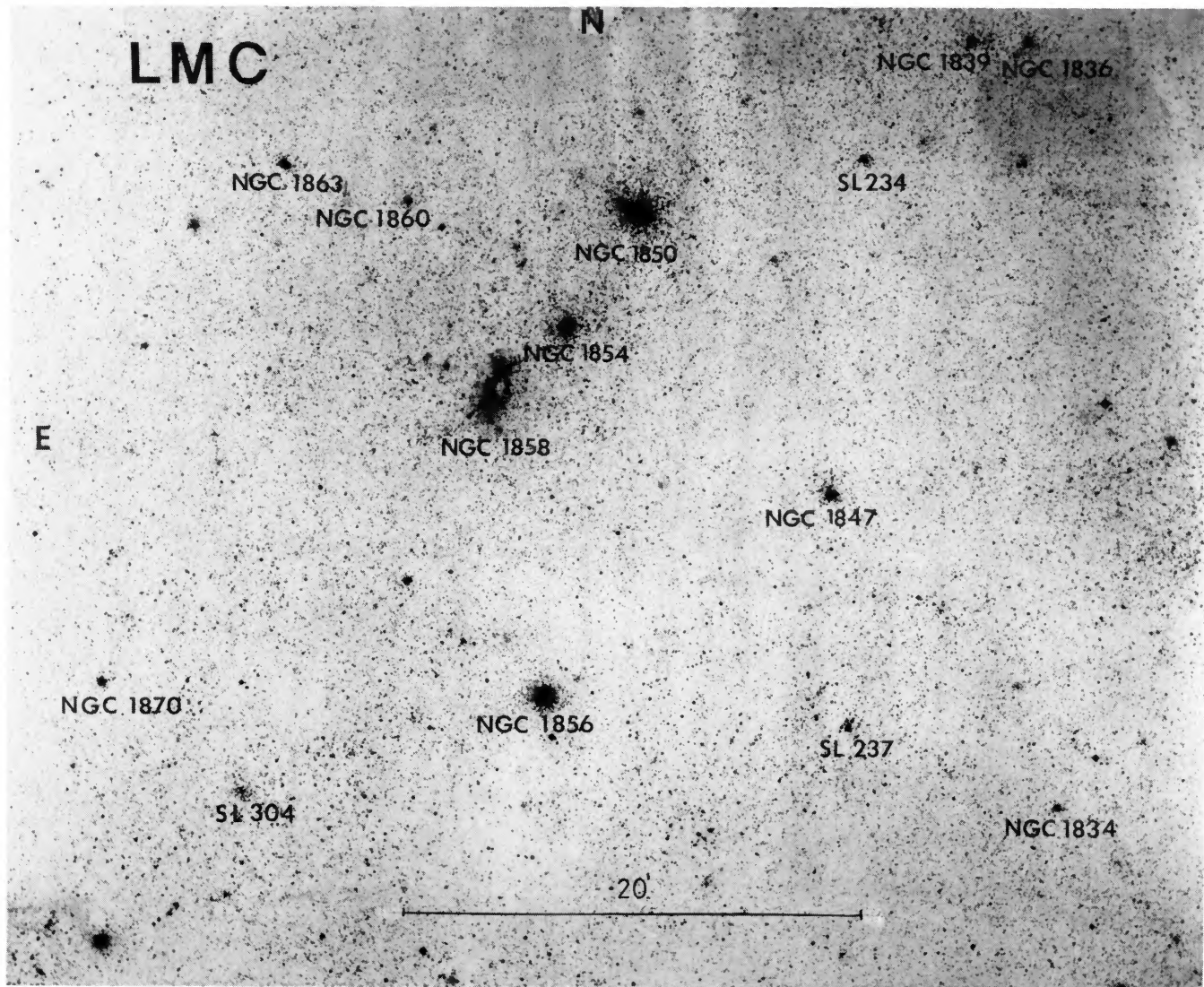


FIG. 2. Finding chart of the studied area. The reproduction is from a 60 min blue plate obtained with the 2.5 m du Pont telescope.

G. Alcaino and W. Liller (see page 372)

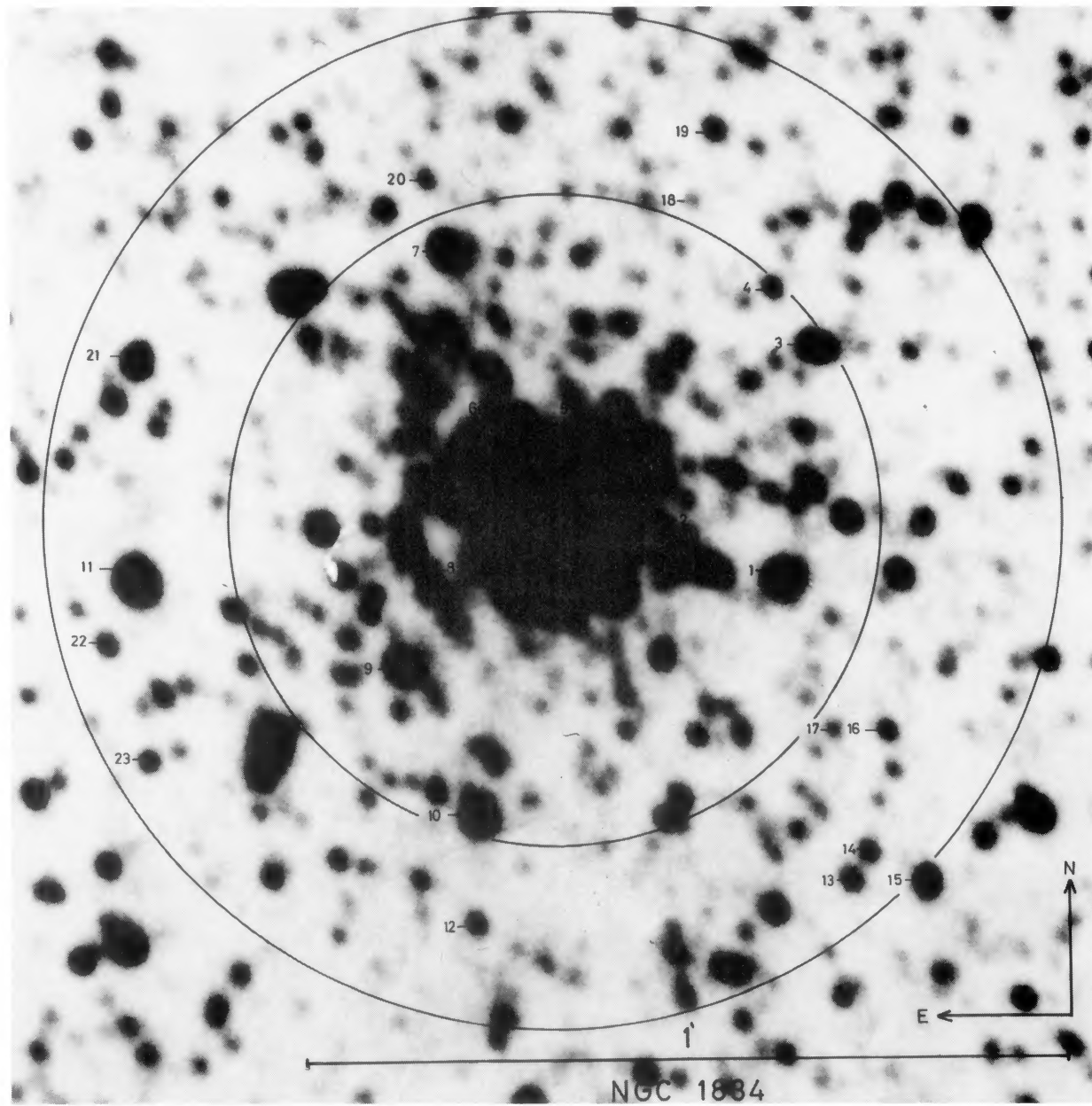


FIG. 4. Finding chart of NGC 1884. Reproduction is from a 14 min blue plate obtained with the 3.6 m ESO telescope.

G. Alcaino and W. Liller (see page 377)

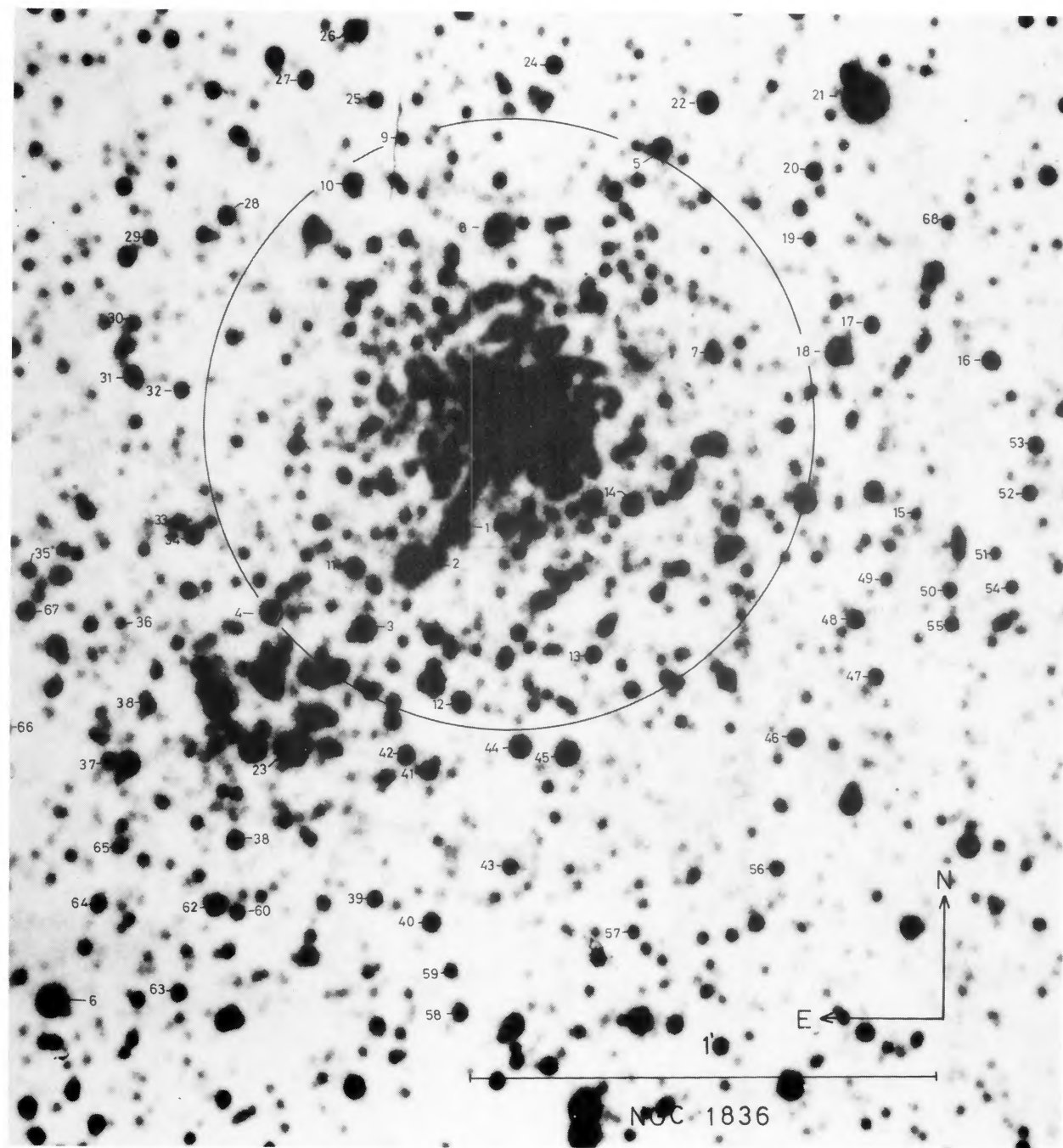


FIG. 6. Finding chart of NGC 1836. Reproduction is from a 14 min blue plate obtained with the 3.6 m ESO telescope.

G. Alcaino and W. Liller (see page 377)

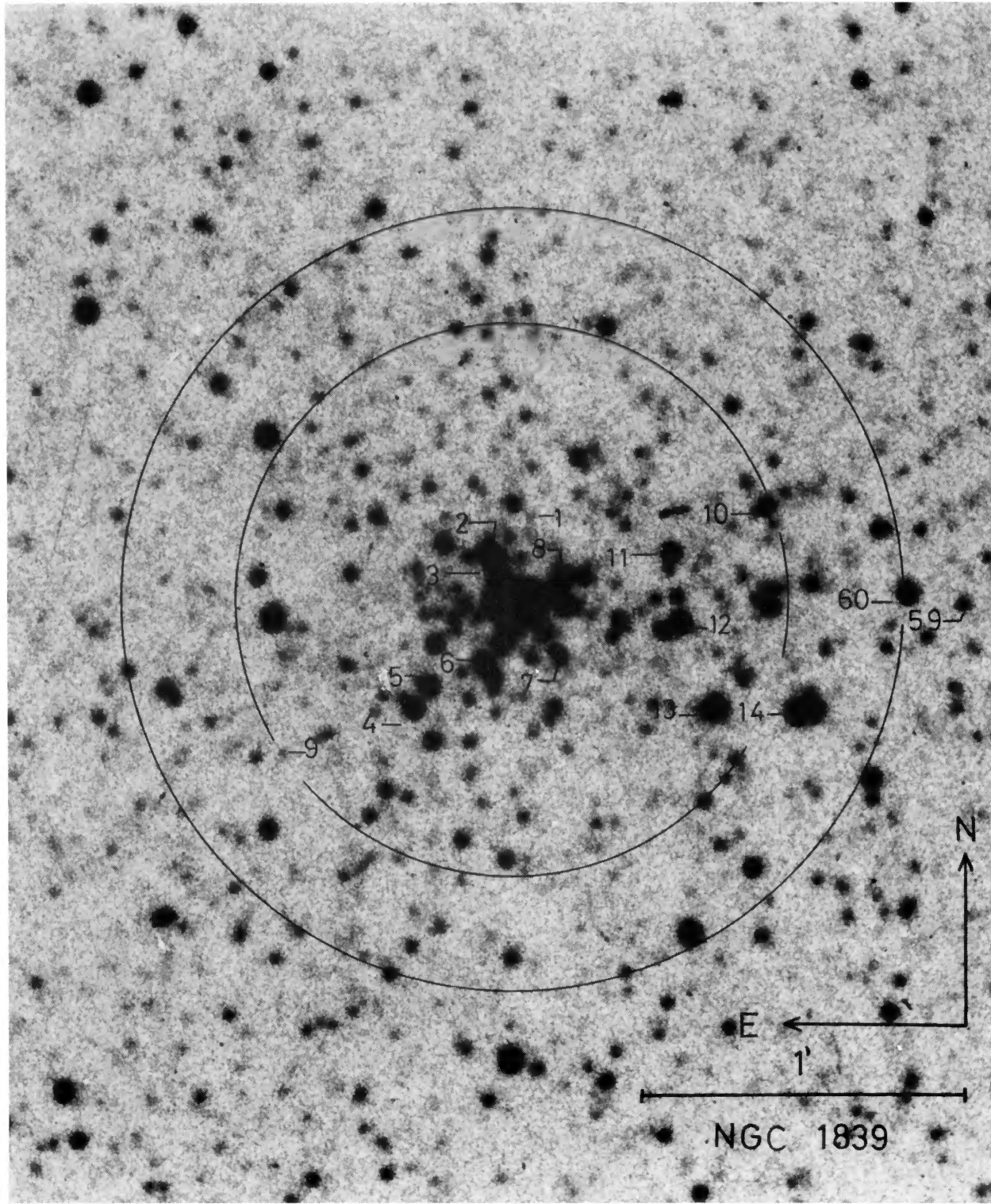


FIG. 8. Finding chart of the inner ring of NGC 1839. Reproduction is from a 15 min blue plate obtained with the 1.5 m Tololo telescope.

G. Alcaino and W. Liller (see page 377)

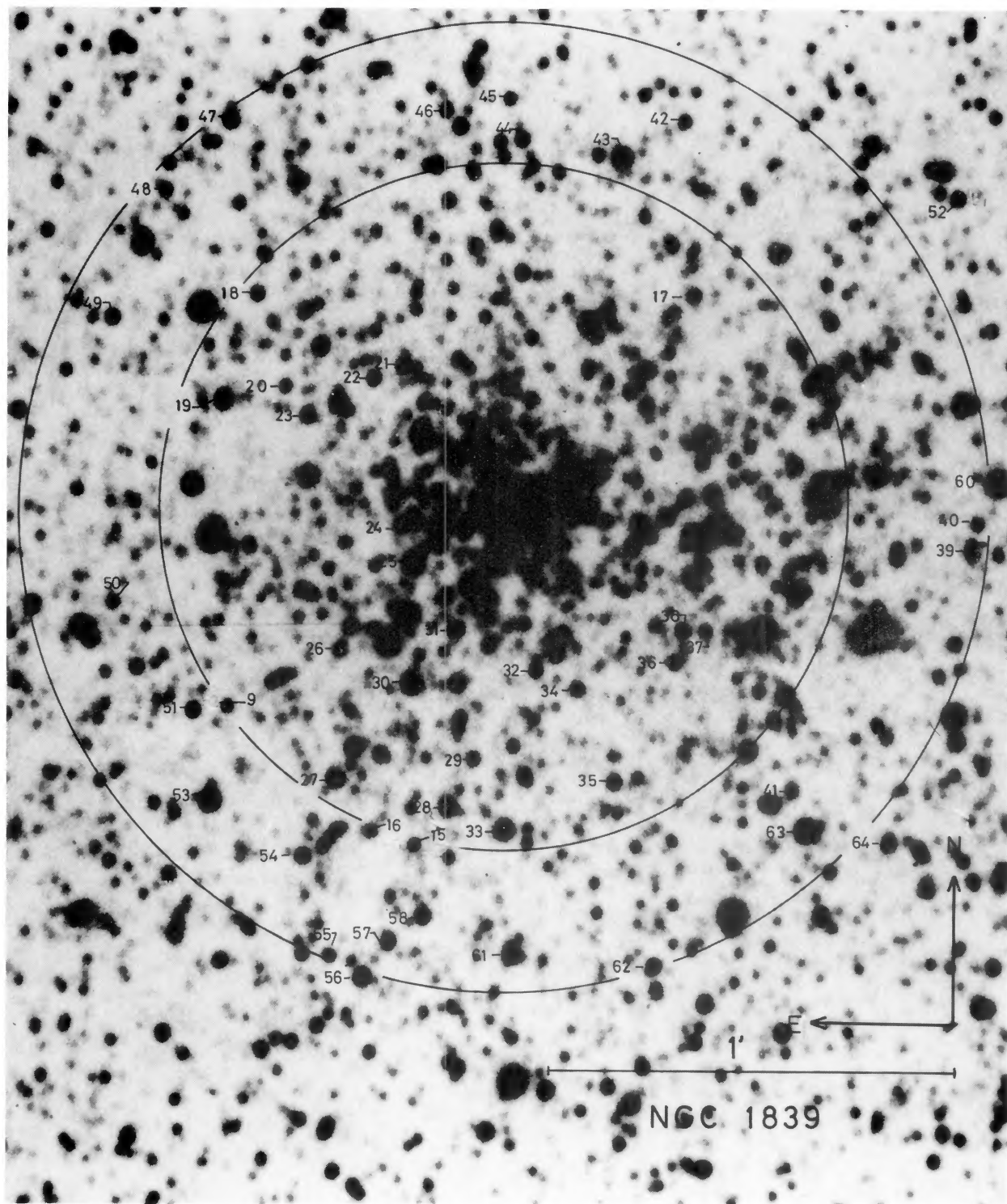


FIG. 9. Finding chart of the outer ring of NGC 1839. Reproduction is from a 14 min blue plate obtained with the 3.6 m ESO telescope.

G. Alcaino and W. Liller (see page 377)

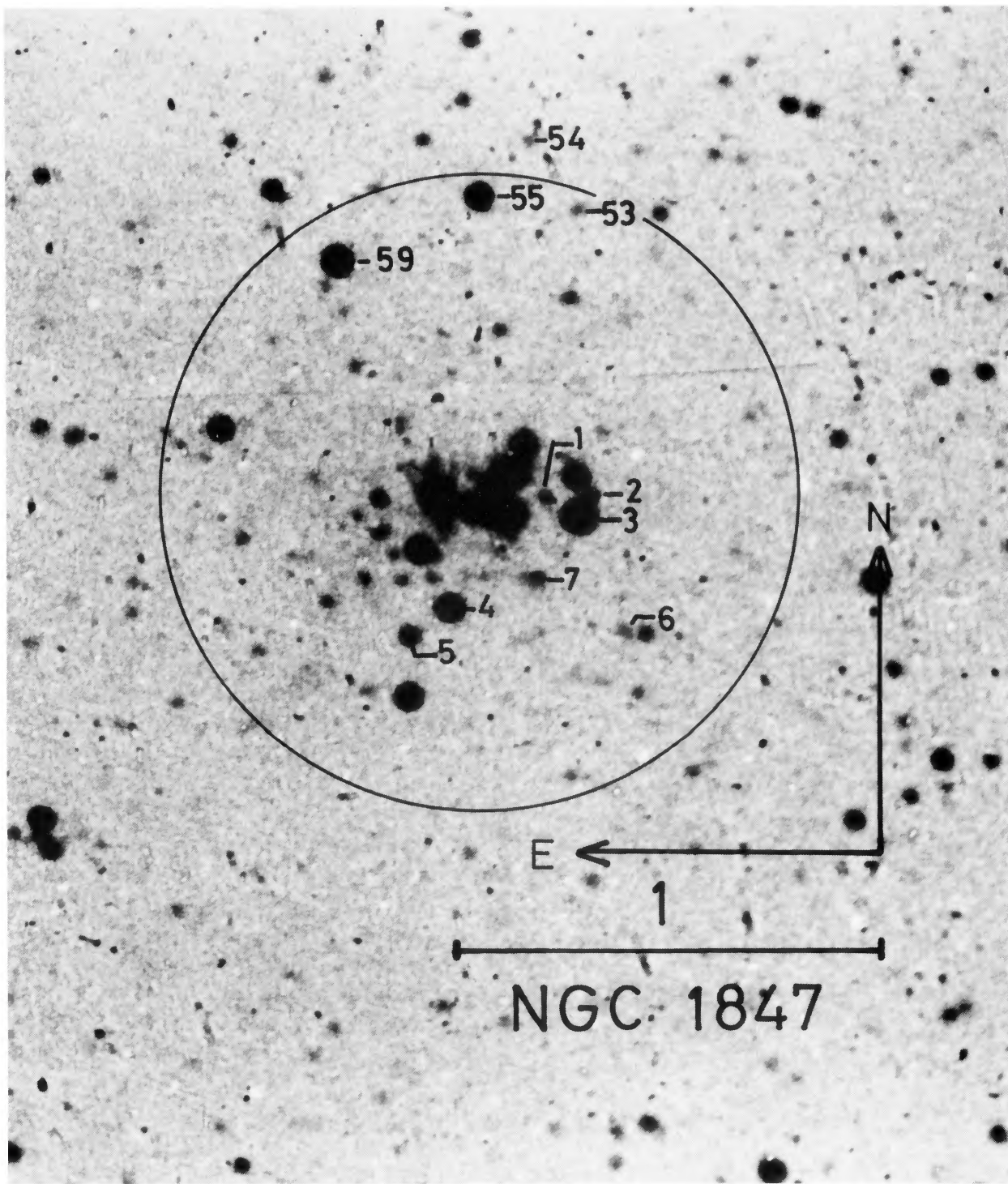


FIG. 11. Finding chart of the inner ring of NGC 1847. Reproduction is from a 10 min infrared plate obtained with the 3.6 m ESO telescope.  
G. Alcaino and W. Liller (see page 377)

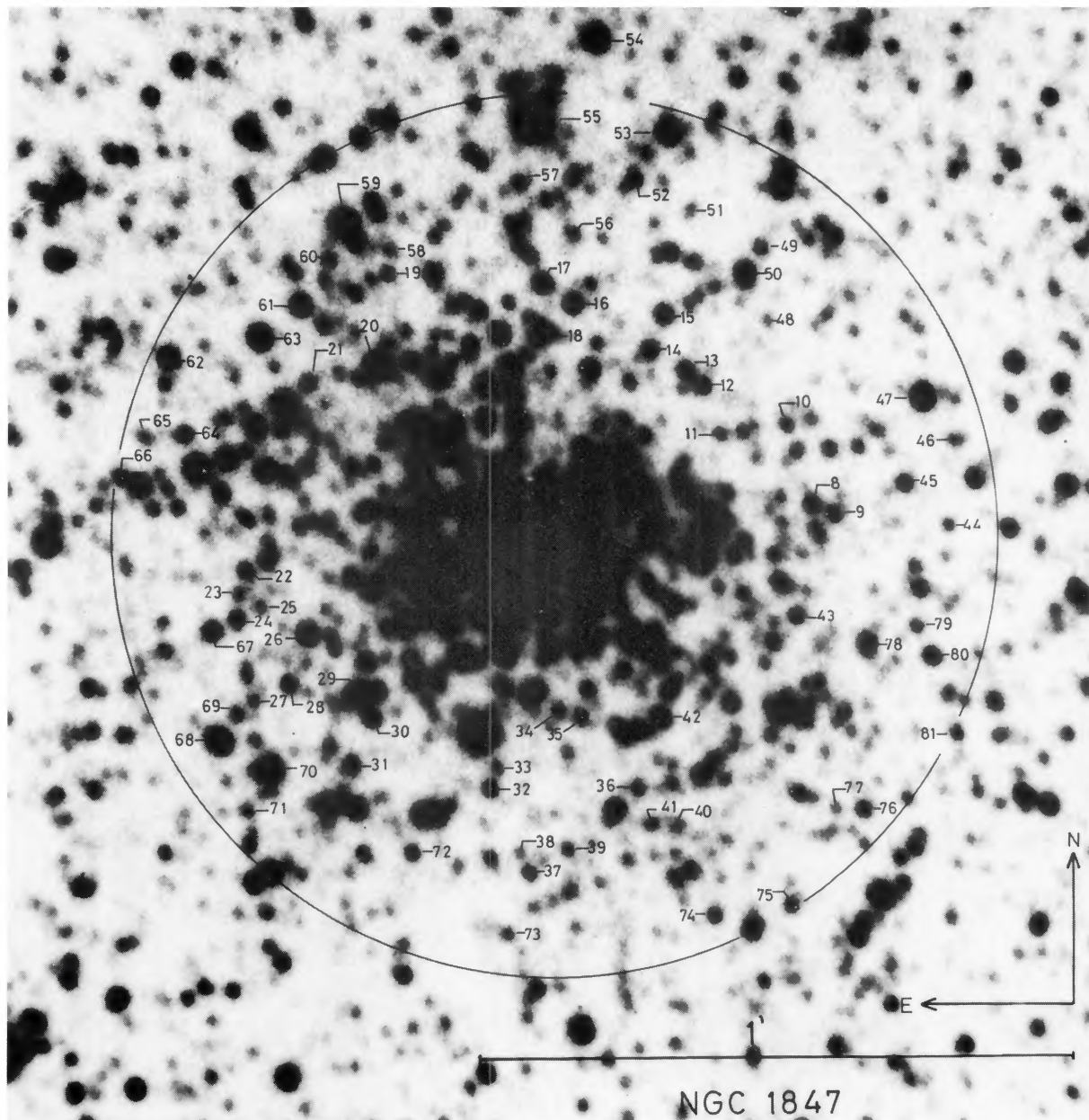


FIG. 12. Finding chart of the outer ring of NGC 1847. Reproduction is from a 14 min blue plate obtained with the 3.6 m ESO telescope.

G. Alcaino and W. Liller (see page 377)

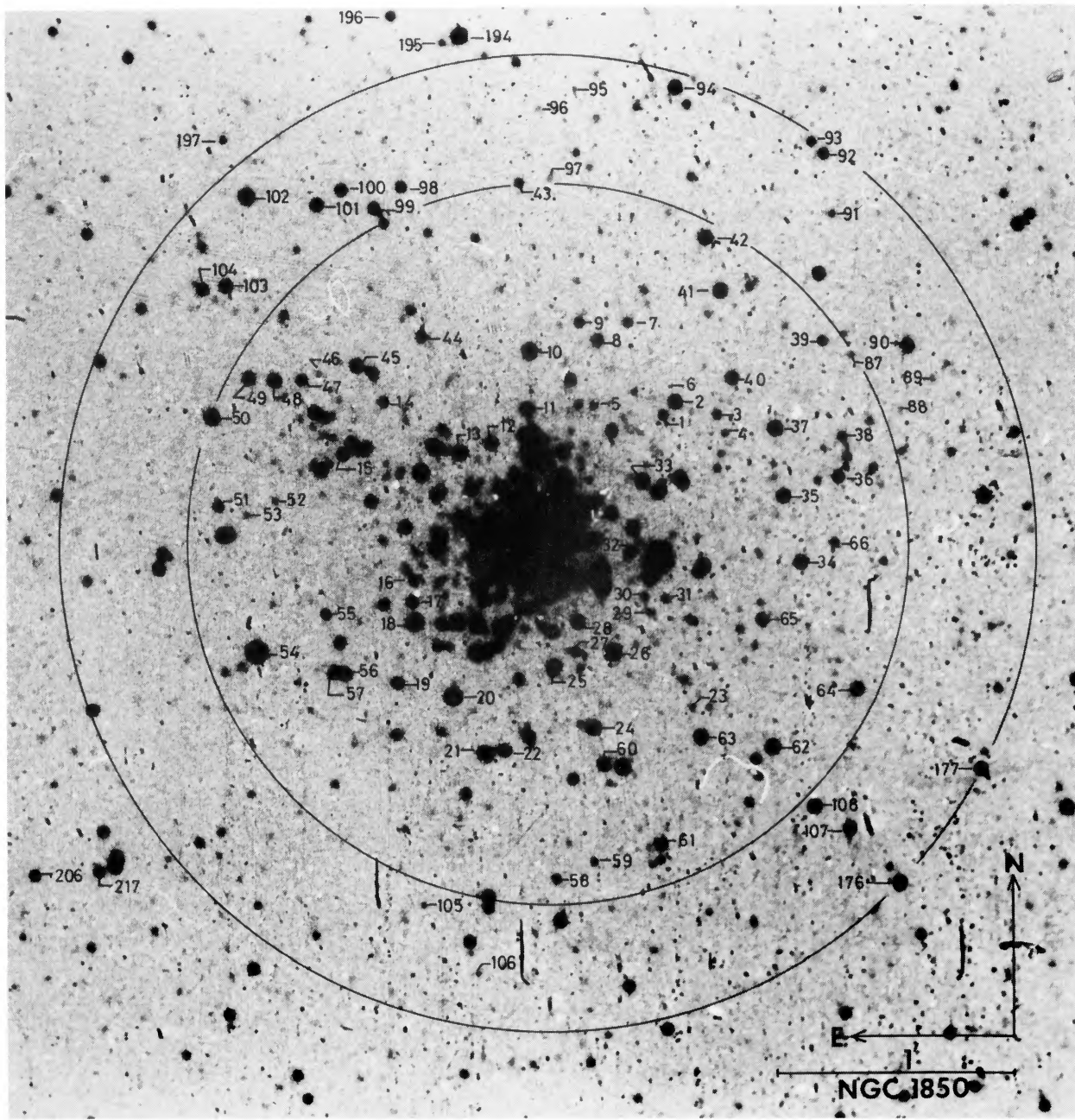


FIG. 14. Finding chart of the inner ring of NGC 1850. Reproduction is from a 10 min infrared plate obtained with the 3.6 m ESO telescope.  
G. Alcaino and W. Liller (see page 377)

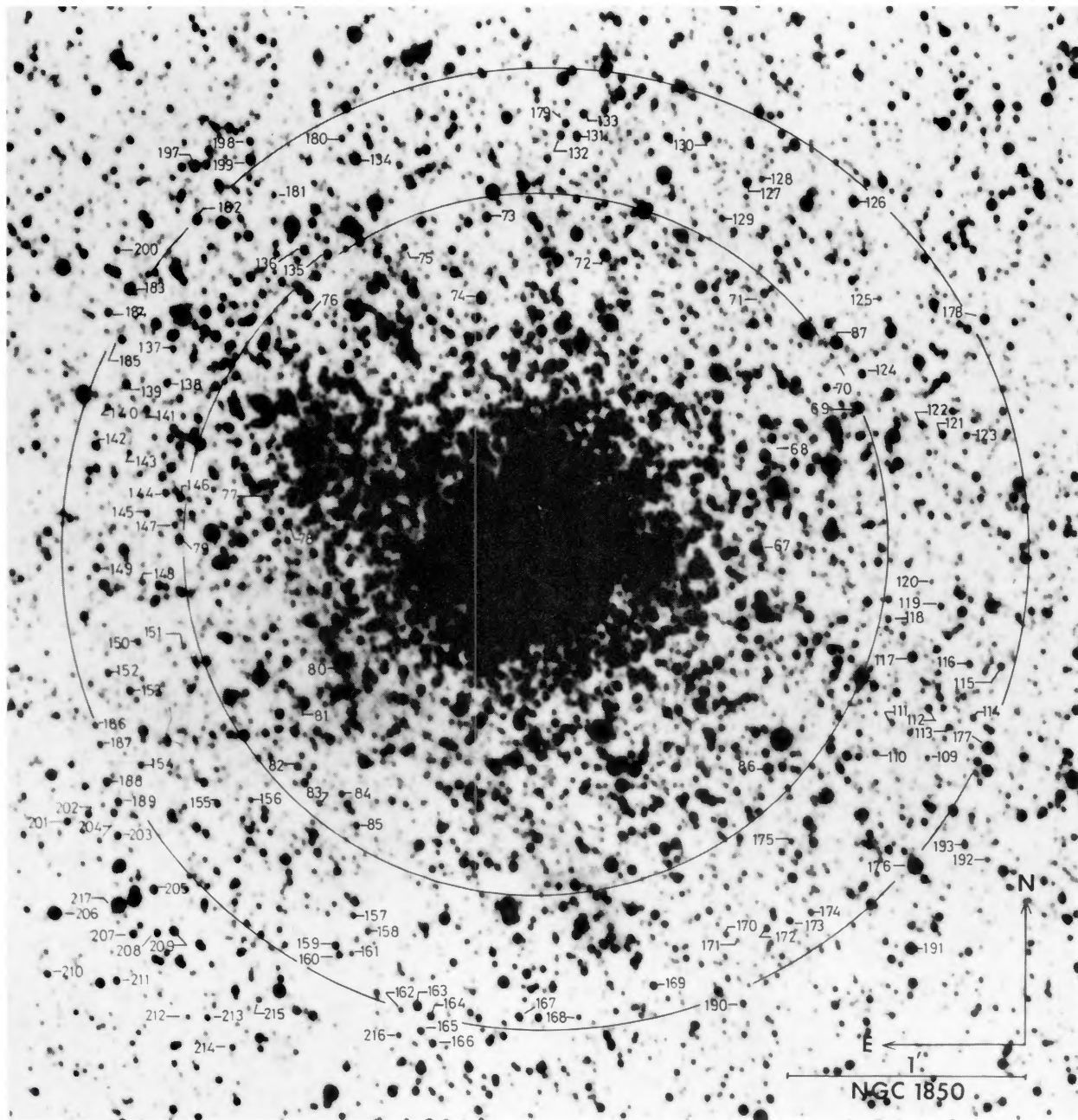


FIG. 15. Finding chart of the outer ring of NGC 1850. Reproduction is from a 14 min blue plate obtained with the 3.6 m ESO telescope.

G. Alcaino and W. Liller (see page 377)

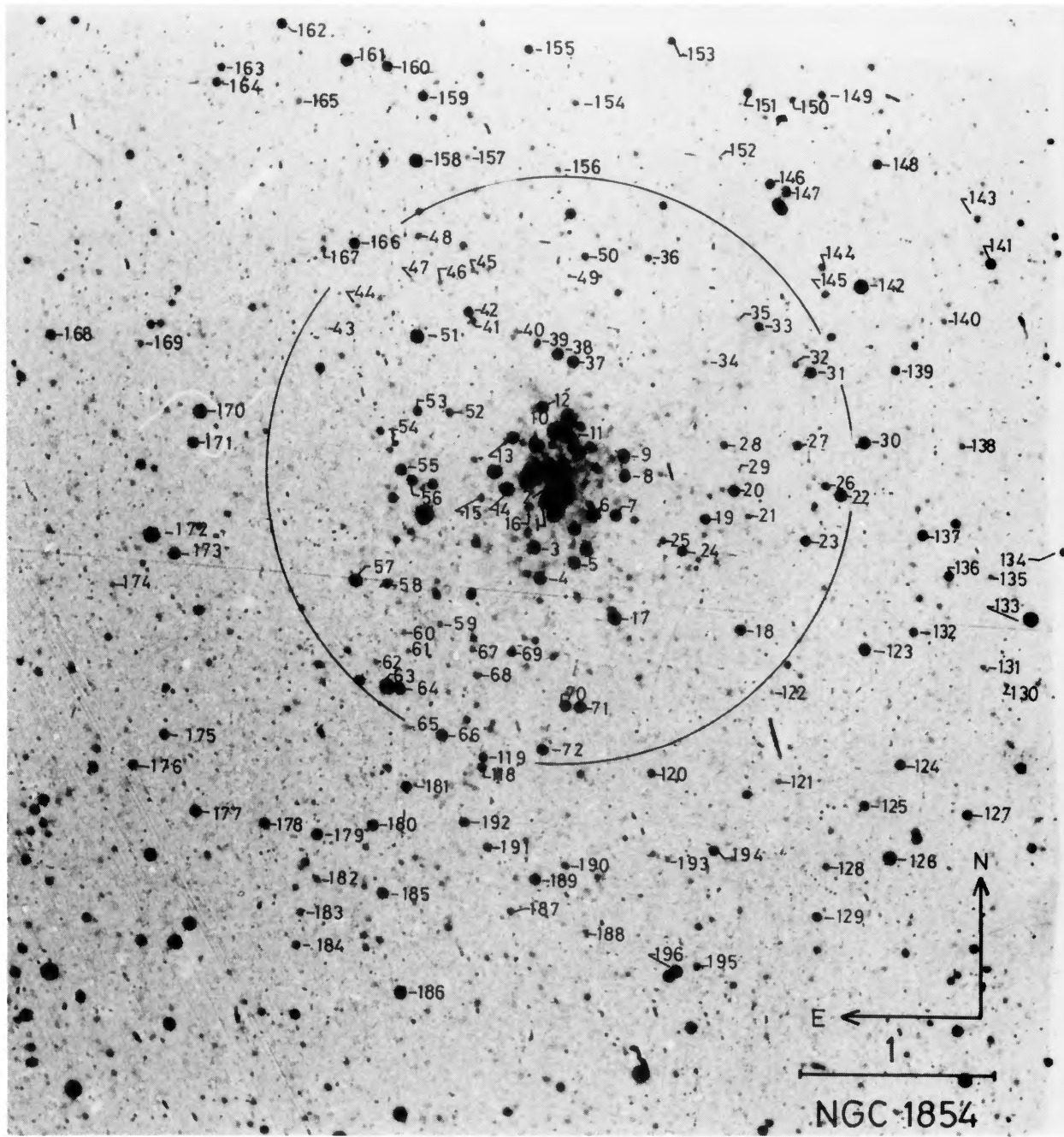


FIG. 17. Finding chart of the inner ring of NGC 1854. Reproduction is from a 10 min infrared plate obtained with the 3.6 m ESO telescope.

G. Alcaino and W. Liller (see page 377)

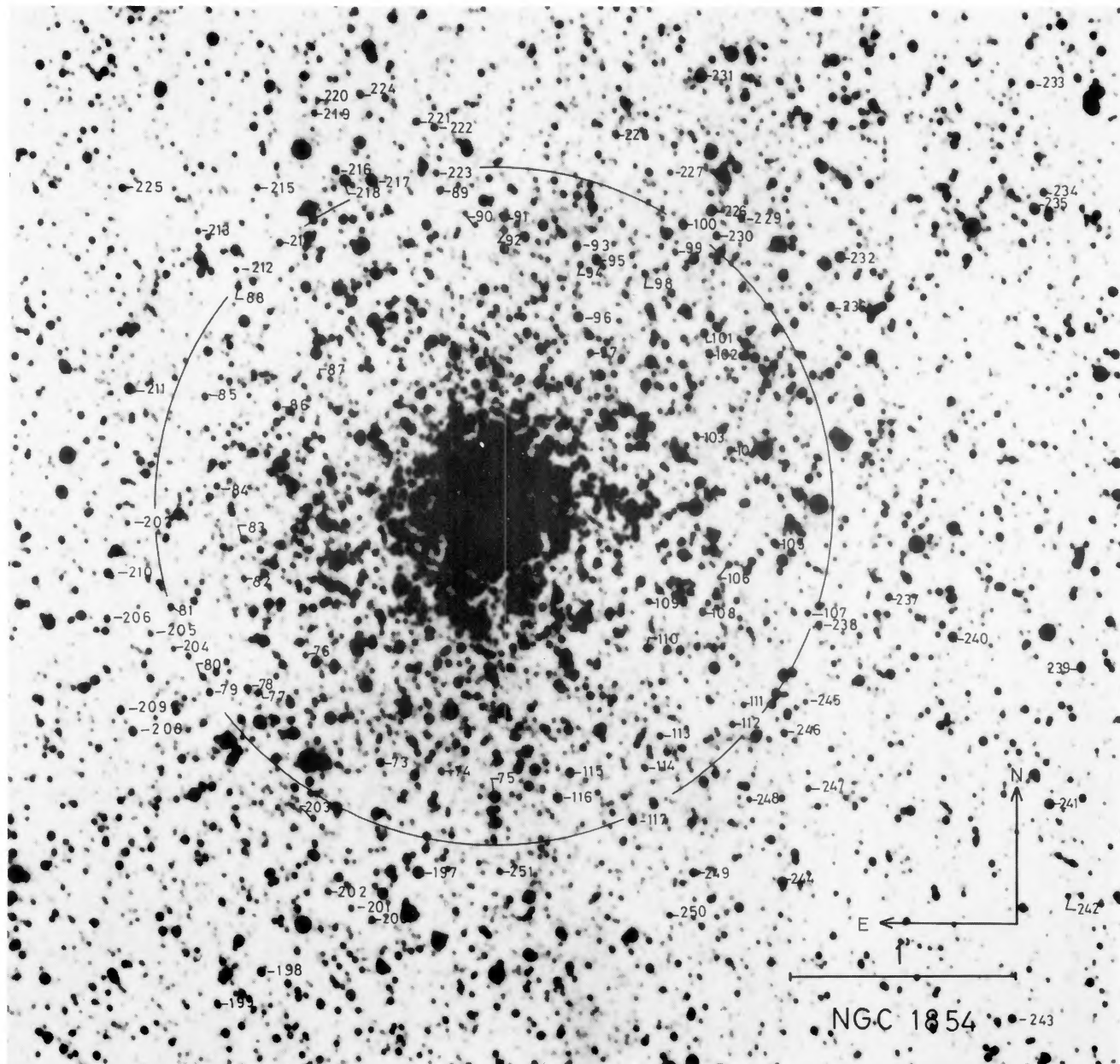


FIG. 18. Finding chart of the outer ring of NGC 1854. Reproduction is from a 14 min blue plate obtained with the 3.6 m ESO telescope.

G. Alcaino and W. Liller (see page 377)

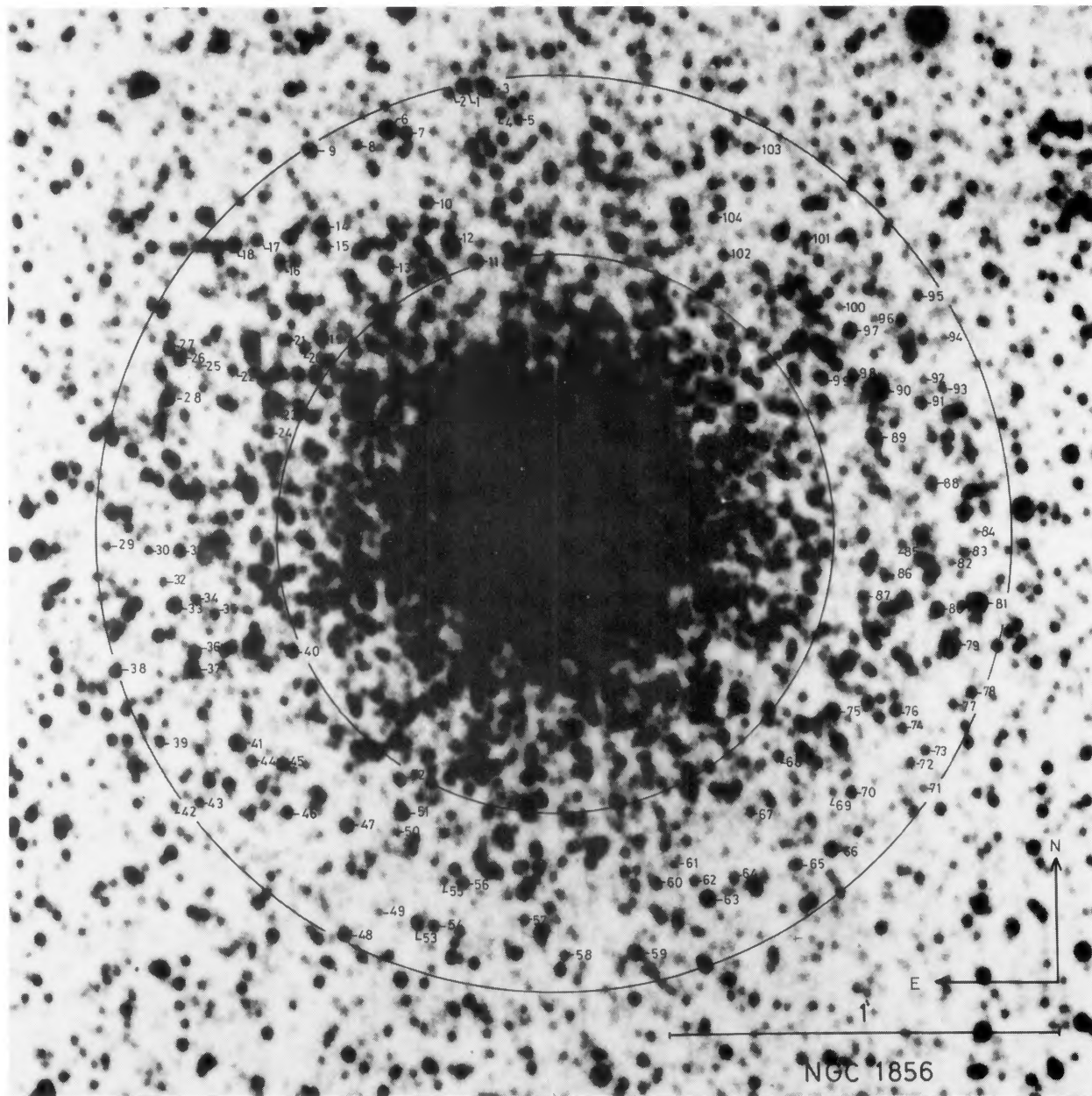


FIG. 20. Finding chart of NGC 1856. Reproduction is from a 14 min blue plate obtained with the 3.6 m ESO telescope.

G. Alcaino and W. Liller (see page 377)

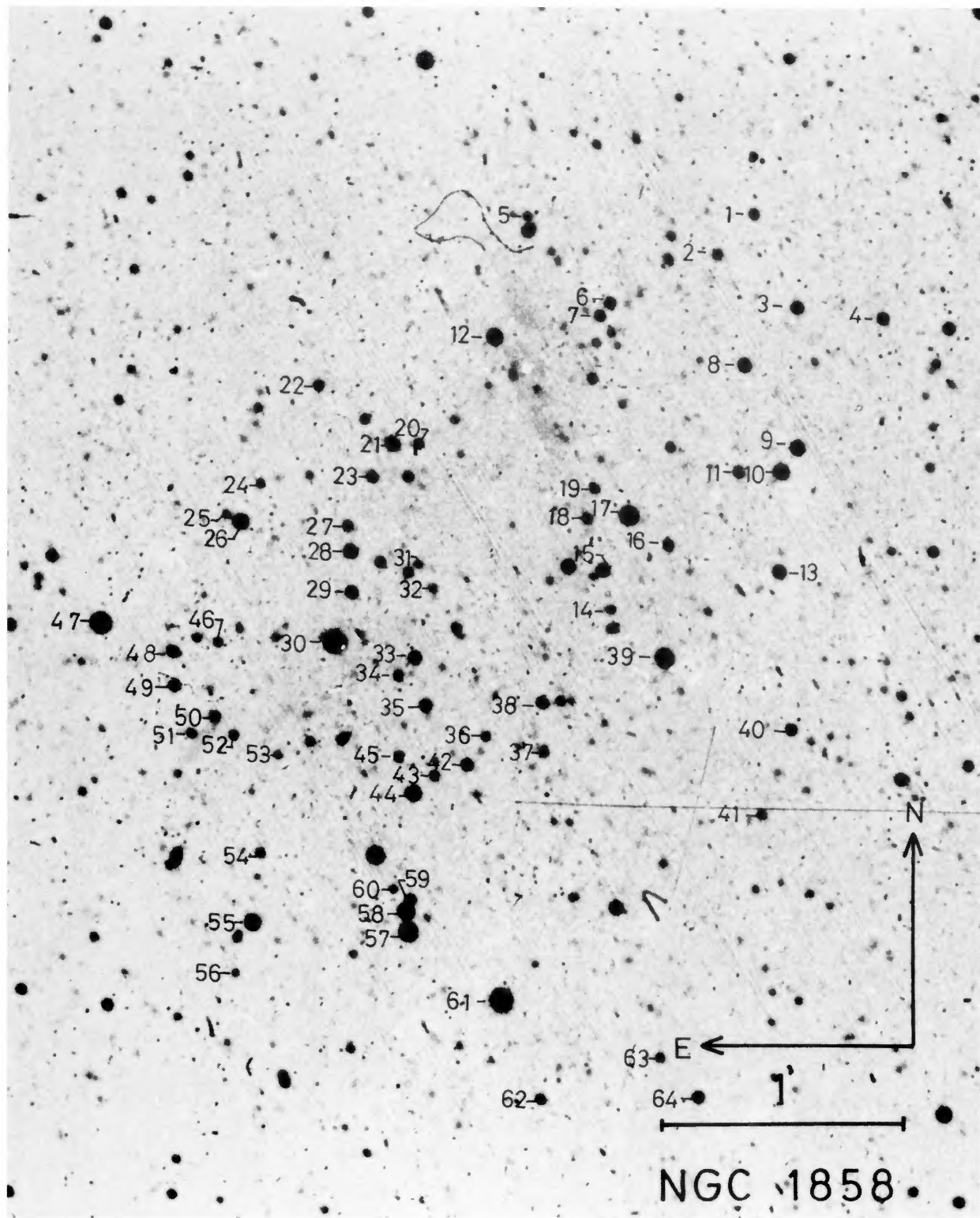


FIG. 22. Finding chart of NGC 1858. Reproduction is from a 10 min infrared plate obtained with the 3.6 m ESO telescope.

G. Alcaino and W. Liller (see page 377)

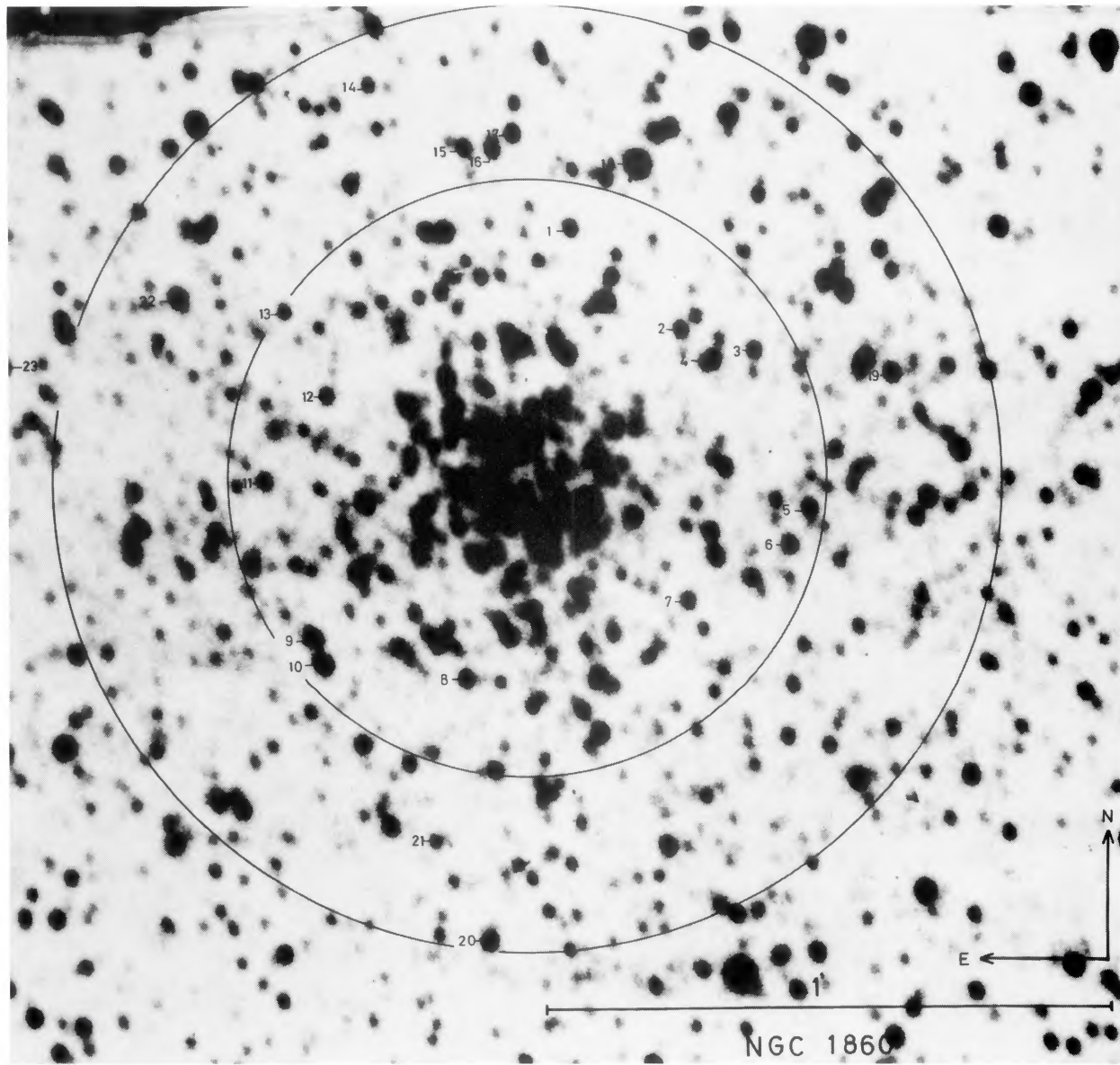


FIG. 24. Finding chart of NGC 1860. Reproduction is from a 14 min blue plate obtained with the 3.6 m ESO telescope.

G. Alcaino and W. Liller (see page 377)

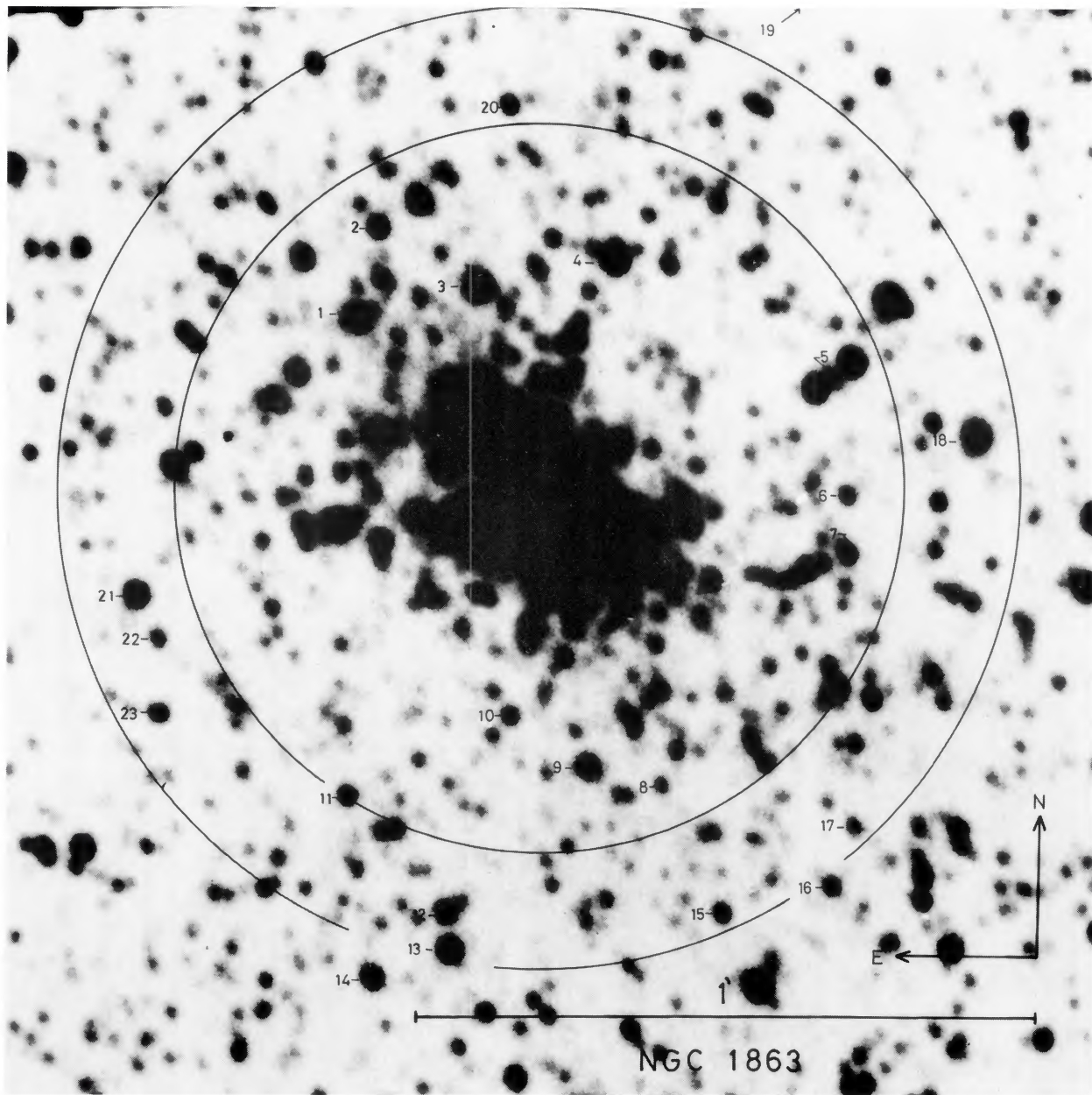


FIG. 26. Finding chart of NGC 1863. Reproduction is from a 14 min blue plate obtained with the 3.6 m ESO telescope.

G. Alcaino and W. Liller (see page 377)

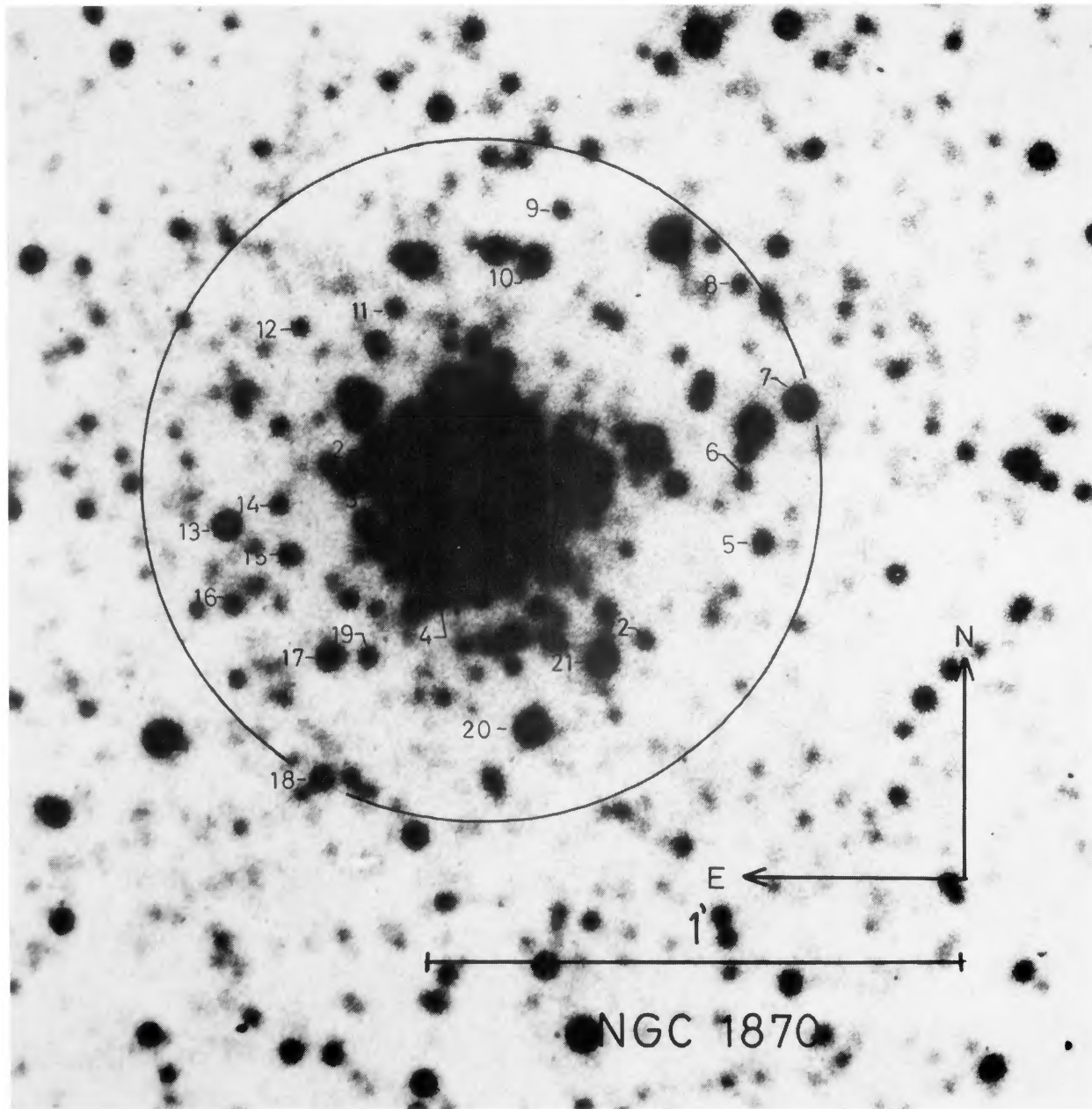


FIG. 28. Finding chart of NGC 1870. Reproduction is from a 15 min blue plate obtained with the 1.5 m Tololo telescope.

G. Alcaino and W. Liller (see page 377)

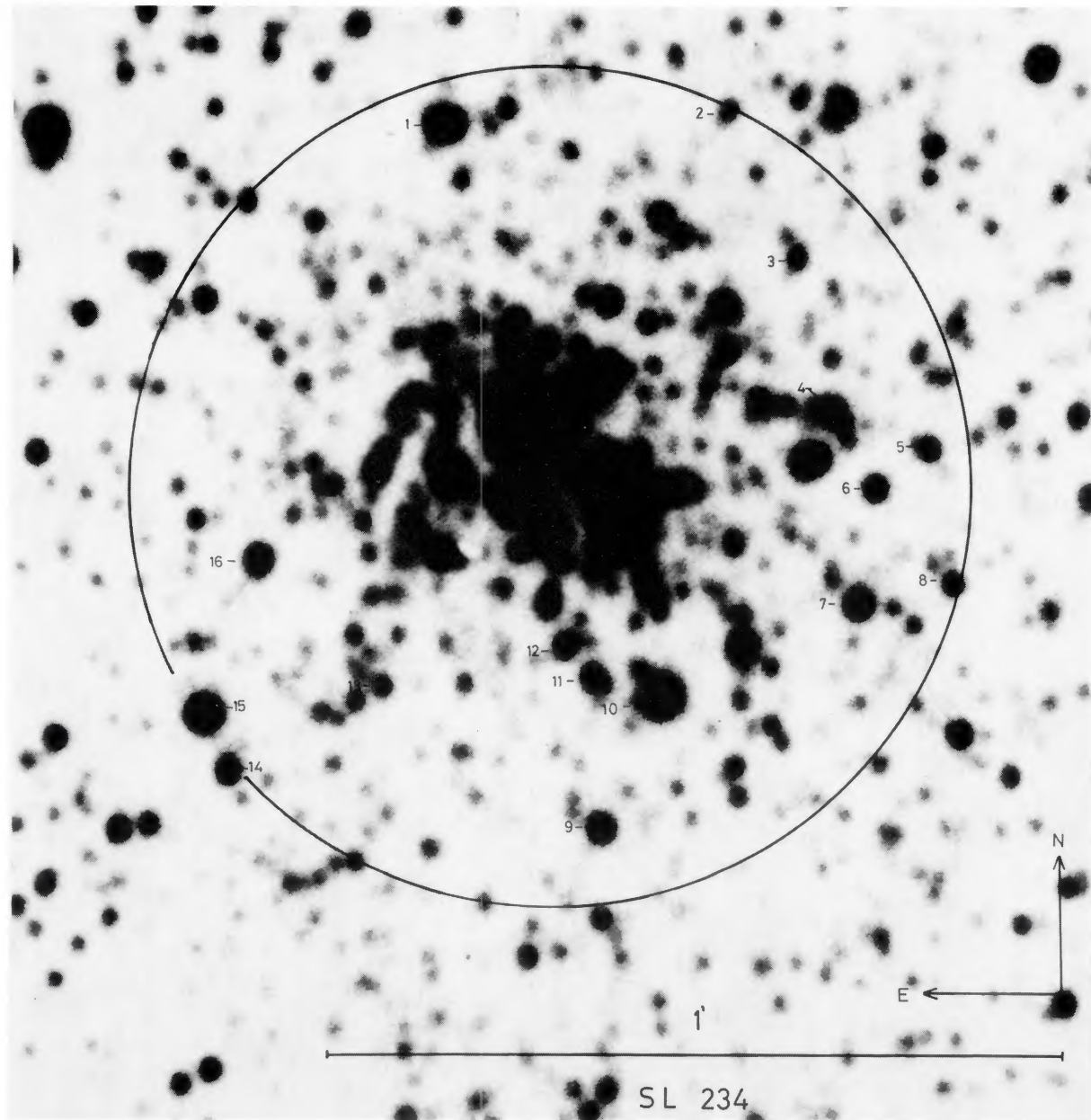


FIG. 30. Finding chart of SL 234. Reproduction is from a 14 min blue plate obtained with the 3.6 m ESO telescope.

G. Alcaino and W. Liller (see page 398)

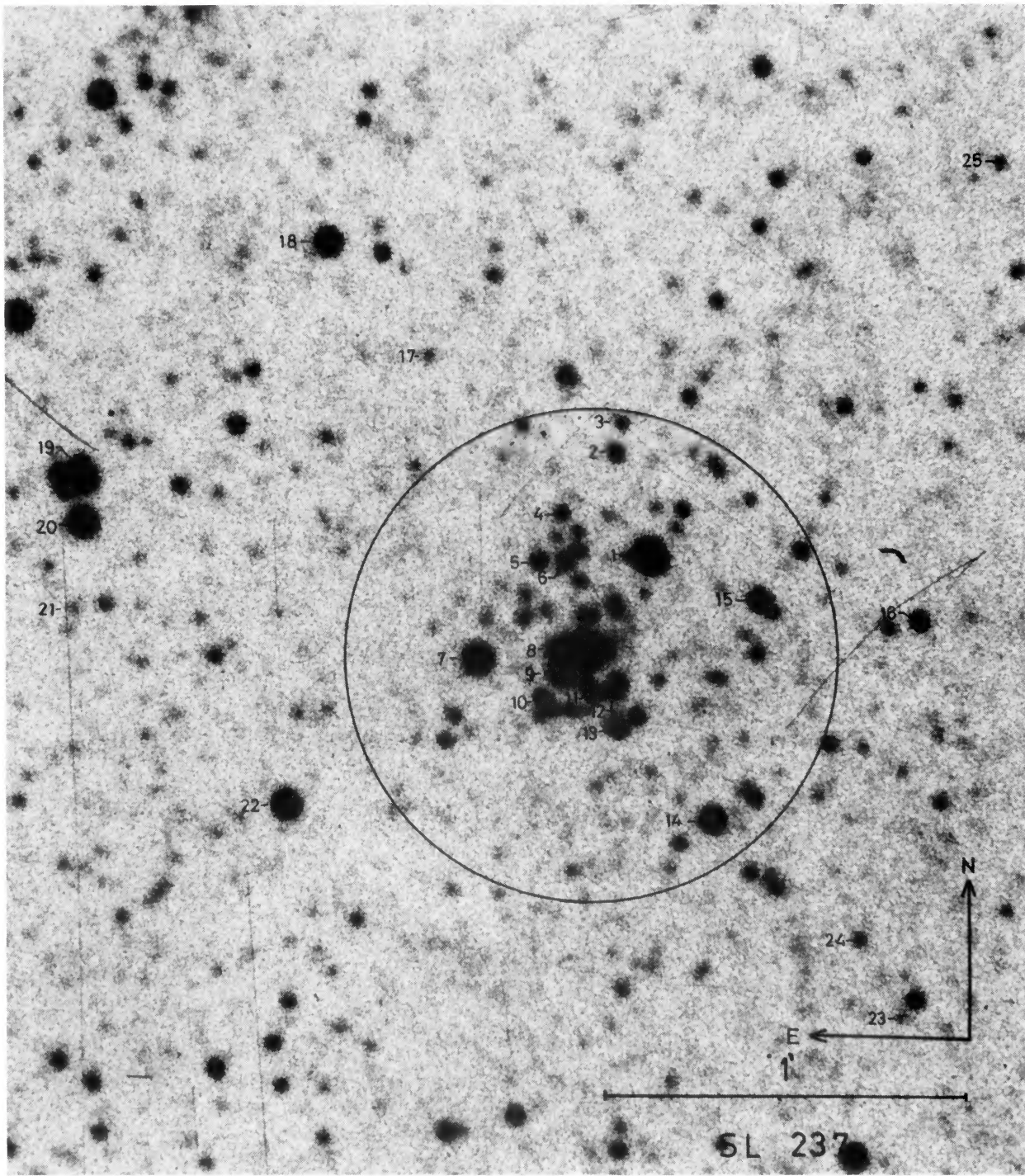


FIG. 32. Finding chart of SL 237. Reproduction is from a 15 min blue plate obtained with the 1.5 m Tololo telescope.

G. Alcaino and W. Liller (see page 398)

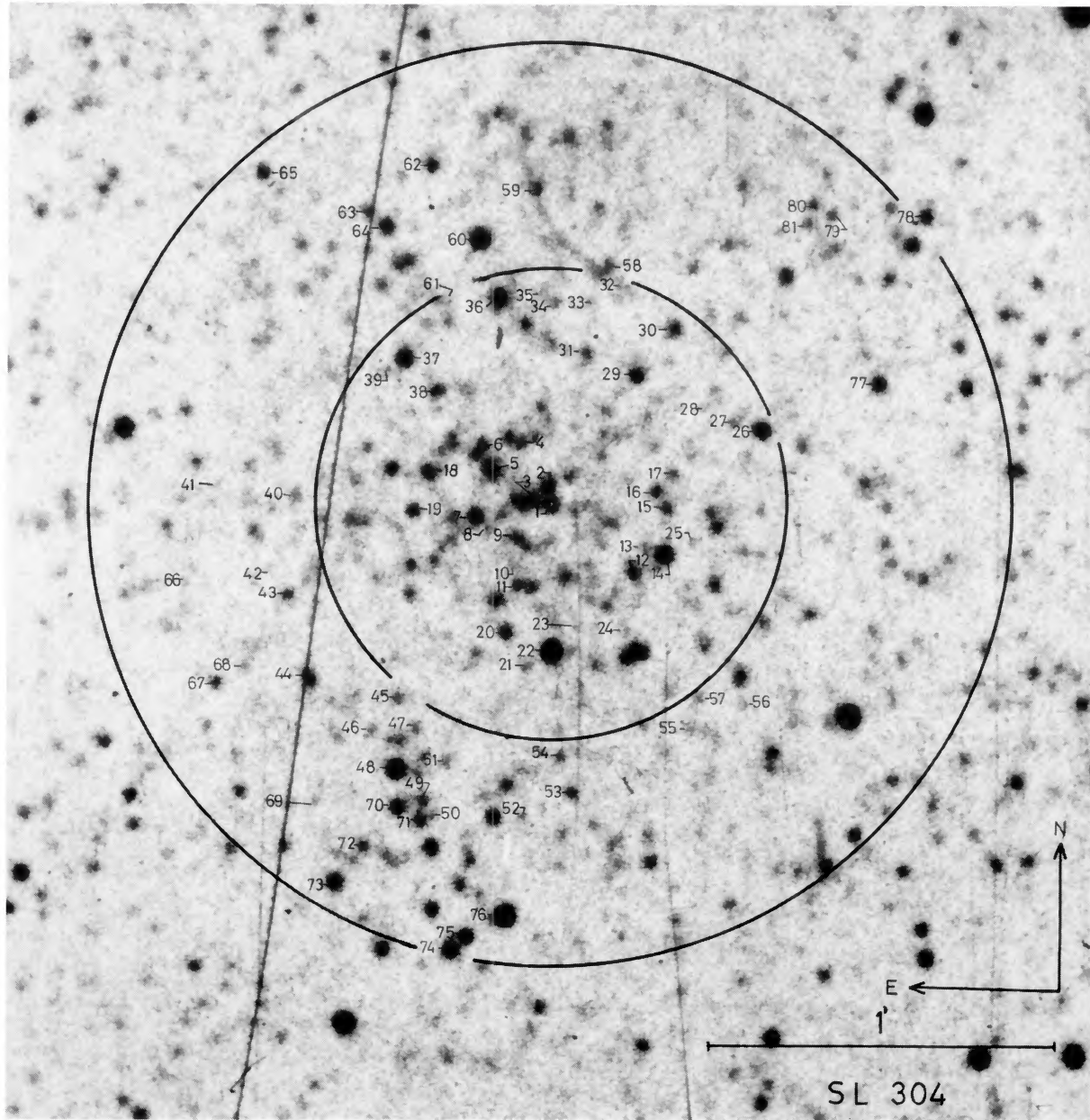


FIG. 34. Finding chart of SL 304. Reproduction is from a 15 min blue plate obtained with the 1.5 m Tololo telescope.

G. Alcaino and W. Liller (see page 398)